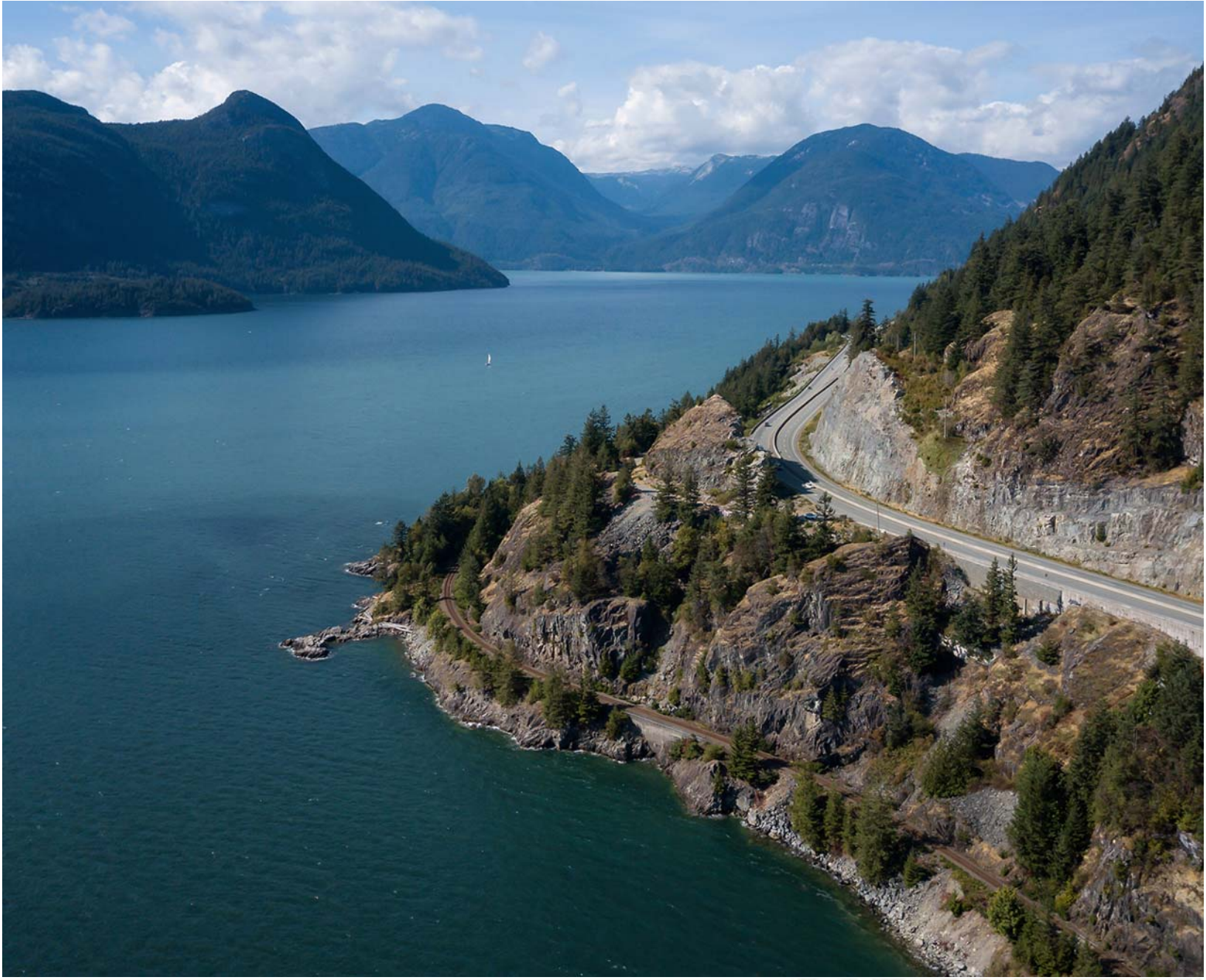

FINAL REPORT

Transit Bus Research

Prepared by:
Suzanne Tylko, Kathy Tang (Innovation Centre, Transport Canada)

Alain Bussières, Marc Duval, François Giguère (PMG Technologies Inc.)

Date: 2022-12-19

Transport Canada

Canada

TABLE OF CONTENTS

LIST OF TABLES

LIST OF FIGURES

EXECUTIVE SUMMARY

This report presents the final results of a multi-year research programme to investigate the crashworthiness of transit buses and to support evidence-informed approaches to enhancing occupant protection.

Five frontal offset transit bus crash tests were conducted with decommissioned buses at 40 km/h and a 40 %, driver-side offset. The test parameters for the two pairs of crash tests (Test 1 & Test2; and Test 3 & Test 4) were matched except for some structural strengthening that was added to the front end of one striking bus from each pair. Test 5 was a non-matched test conducted to supplement the dataset, and study the influence of seatback geometry.

The strengthening of the bus reduced the intrusion into the driver occupant space and resulted in a redirection of load to the upper body and a reduction of loading to the legs of the driver. The strengthening resulted in negligeable changes in peak acceleration (<2 g) of the passenger compartment of the bus. In all tests the acceleration of the striking bus never exceeded 10 g. All dummies placed in the passenger compartment of the striking bus (with the exception of a restrained dummy in a wheelchair) either impacted the seat in front with the head or were ejected from the seat.

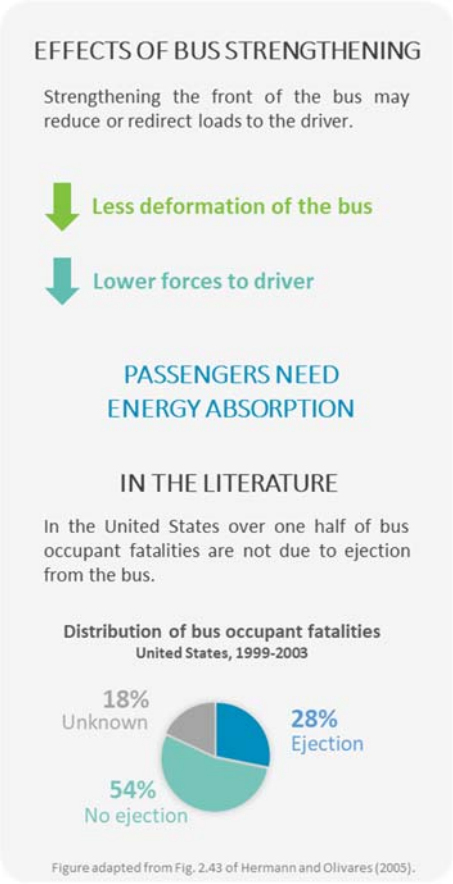

A sled buck representing a section of a transit bus passenger compartment was constructed so that, through controlled sled testing, the dummy responses could be examined in greater detail. The similarity of dummy motions between the bus crashes and the sled tests suggests that the dummy motions observed in the buses can be reproduced on the sled. Crash pulse severity, the dummy posture and seat placement (inboard vs. outboard) were all found to influence the response of the dummies.

The sled data was used by the University of Waterloo to develop and validate a finite element model to compare the simulated motions of the human body model to the physical dummies. Impact of the neck with the handrail which was observed in the physical testing cannot be detected by the instrumentation of the physical dummy. Simulation of the neck impact with the human body model however identified a risk of injury to the larynx.

The study demonstrates that there are important potential opportunities to improve the protection of occupants in low to moderate severity bus collisions. Modifications to the structure of the bus will not be sufficient to reduce the risk of head impacts. Resources should instead be directed towards optimizing the interior of the bus to provide better energy absorption when the head strikes occur to improve passenger protection in the most common transit bus collisions.

1. INTRODUCTION

In pre-pandemic Canada, 12.4 % of commuters used public transit[1]. Ridership on transit buses had been increasing since the mid-1990s[2], increasing by an estimated 2.4 %, or approximately 50 million passengers between 2017 and 2018[3]. The incidence of fatality or serious injury associated with transit bus crashes remains low; the United States National Highway Traffic Safety Administration (NHTSA) reported that in 2017, 0.4 % of vehicles involved in fatal crashes were buses[4]. In 2013, a double-decker bus collided with a passenger train. The collision resulted in 5 occupant ejections, 6 fatalities, and 34 injuries[5]. The collision was investigated by the Transportation Safety Board (TSB). As part of the report, the TSB suggested that "a more robust front structure and crash energy management design might have reduced the damage to the bus and prevented the loss of a protective shell for the occupants"[5]. In 2015, the TSB issued the recommendation that "the Department of Transport develop and implement crashworthiness standards for commercial passenger buses to reduce the risk of injury"[5].

In response to the TSB recommendations, Transport Canada launched a multi-year research programme to investigate the crashworthiness of transit buses and to provide scientific evidence in support of possible future regulatory initiatives. Specifically, the research programme was designed to examine the effects of structural stiffness and energy management on the protection of transit bus drivers and passengers during frontal crashes.

The protection of passengers during a crash relies on striking a balance between the strength of the vehicle structure and the dissipation of the crash energy. A very stiff shell for example, may remain intact and prevent ejections but the energy that would have been dissipated during the crushing and destruction of that shell must somehow be directed away from the occupants. Energy management becomes all the more challenging for unrestrained passengers (without seat belts) who may be seated or standing. These principles of occupant protection apply to all vehicle types.

An important and necessary part of the research programme involves the interpretation of dummy responses within the context of the transit bus occupant space. Crash test dummies were designed for the monitoring of passenger car safety regulations. In a passenger car crash test, the dummies are displaced forward but remain seated and mostly upright, contained by multiple safety systems such as seatbelts, airbags, and knee bolsters. The implications of the non-humanlike, stiff, seated posture of the dummy may be less significant in this environment. However, in a transit bus, where the dummy movements are not restrained, the stiffness of the dummies can have a great influence on what the head and other body parts might strike and the interpretation of those responses. Additional tools are required to help improve the accuracy of injury risk prediction.

This report presents the results of five full-scale transit bus crash tests. It describes the fabrication of a sled buck that is representative of a transit bus section; and presents the results of a collaborative initiative with the University of Waterloo to develop a numerical model based on the test data. To our knowledge, Transport Canada is the only organization to have conducted full scale transit bus crash tests of this type. The data obtained from these crash tests are essential for the development and validation of the sled test programmes and for future modelling studies.

2. OBJECTIVE

The objective of this multi-year transit bus research programme is to investigate the crashworthiness of transit buses in order to support evidence-informed regulatory initiatives.

3. CRASH TESTS

3.1 METHODS

A total of five transit bus crash tests were conducted. For reasons of availability and cost, these buses were used instead of double decker buses. In each crash test, the driver side of a moving bus (Striking Vehicle) impacted the right rear corner of a stationary bus (Target Vehicle). The impact speed of the Striking Vehicle was 40 km/h and the overlap at impact was 40 %, as shown in Figure 1.

Test 1 and Test 2 were conducted with two decommissioned New Flyer D40i buses purchased from the City of Ottawa; In Test 1, which served as the baseline or reference test, both buses were in their original condition upon delivery. In Test 2, the same vehicles were used, but the positions were reversed, i.e., the Target Vehicle in Test 1 became the new Striking Vehicle.

In Test 3 and Test 4, Test 3 served as the baseline, the Striking Vehicle in Test 4 was reinforced. Since Test 3 and Test 4 were conducted with four identical decommissioned New Flyer B40 LF buses there was no need to re-use a bus as had been done previously.

Test 5 was a single test conducted with two identical Nova Bus LFS buses. These buses were built on a completely different platform. While all buses in the test sample shared the same exterior dimensions (40 feet long and 102 inches wide), the LFS model did not feature a second door in the middle of the bus and offered less seating space at the rear of the bus. The layout of the seats was different but most importantly the characteristics of the seats and the height of the seatbacks are different from the sample of New Flyer buses.

Figure 1: Front and top view of vehicle alignment for Test 1 and Test 2 (top) Test 3 and Test 4 (bottom).

3.1.1 Structural Reinforcement of Striking Vehicle Test 1 and Test 2/ Test 3 and Test 4

Once Test 1 and Test 3 were completed, the front of the striking vehicle was inspected and the damage was measured and documented. Structural reinforcements were proposed and shared with the bus manufacturer for consultation. Structural reinforcements, shown in Figure 2, were added to the Striking Vehicle of Test 2 and Test 4. Materials used included square A500 steel Hollow Structural Section tubes (HSS) and flat steel plates of varying size and thickness. The three key elements of the reinforcements were located at:

1. The window frame: 2"x2" HSS tubes were installed around the window frame and diagonally across the window;
2. The service panel: 2"x2" HSS tubes were installed around the service panel;
3. The bumper: an 8' long 2"x10" HSS tube was installed behind the original bumper.

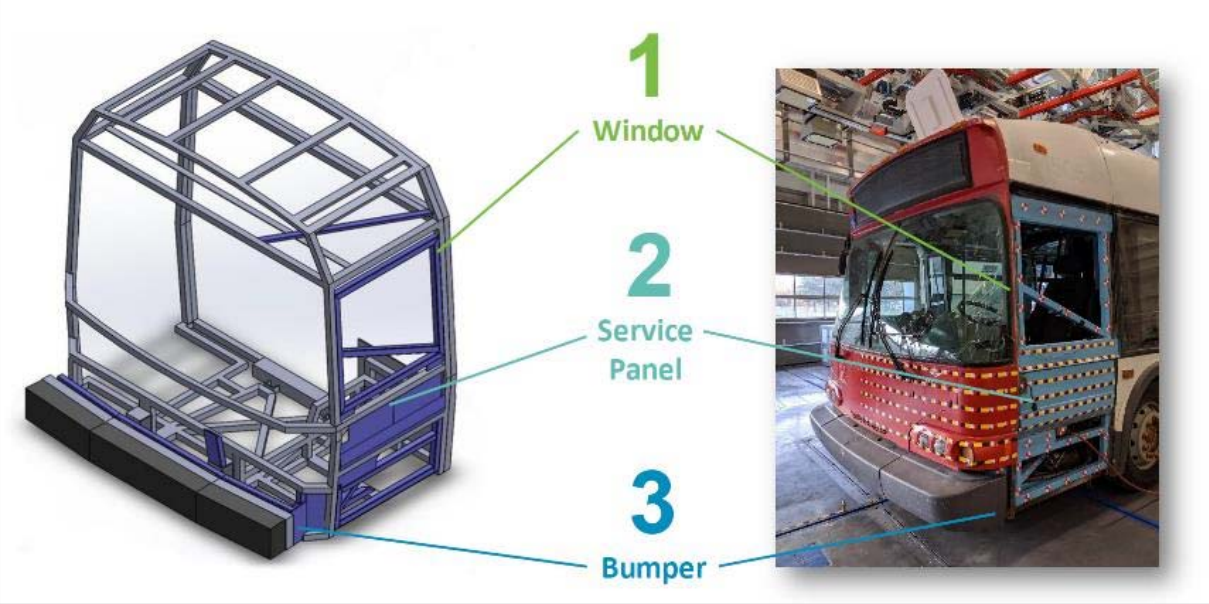

Figure 2: CAD drawing (left panel) and photo (right panel) showing the key reinforcements added for Test 2. In both images, the reinforcements are shown in blue.

To the greatest extent possible, the reinforcements added to the Striking Vehicle in Test 4 were comparable to the reinforcements added to the Striking Vehicle in Test 2. There were three key differences in the reinforcements added for Test 4:

1. The tube installed at an angle in the base of the bus, in the opening underneath the service panel (Figure 2). The angle of this bar could not be matched exactly in the new bus due to the differences in construction between the two models. The points of attachment represent equivalent parts of the structures of each bus.
2. The 2"x10" tube behind the bumper was exchanged for a plate because the new bus had less space to work with behind the bumper than the previous bus and fitting an identical tube was not possible.
3. Below the window, covered by the service panel, the horizonal support that was previously reinforced was absent in the new bus so an additional tube was installed to take its place

3.1.2 Bus Deformation Measurements & Instrumentation

To quantify the deformation of the bus, targets were placed across the front of the striking vehicle, and the pre- and post-test positions of each target were recorded to quantify their displacements in three dimensions (3D). The longitudinal components of the displacement measurements were used as indicators of intrusion.

The deceleration/acceleration responses of the striking and target buses were recorded using accelerometers at the approximate centres of gravity of the vehicles. On the striking bus, accelerometers were also placed under each seat occupied by a dummy.

3.1.3 Dummy Placement

A total of 11 dummies were installed at various locations on-board the striking vehicle for Test 1, Test 2, Test 3 and Test 4, and 18 dummies were on board in Test 5. Two additional dummies were placed at the rear of the Target Vehicle in Test 3 and Test 4. The lay outs for dummy placement are shown in Figure 3 where the upper schematic is for Test 1 and Test 2, the bottom is for Test 3 and Test 4. Dummy positions were matched for each pair of tests, this included dummy serial number and placement of arm, leg and feet positions. Test 5, which was not part of a paired comparison is shown in Figure 4.

The dummies were representative in size of an average size man (Hybrid III and WorldSID 50th percentile), a small woman or teenager (Hybrid III 5th percentile), a 10-year-old child (Hybrid III), and a six-year-old child (Hybrid III and/or Q6). Each dummy was instrumented to record head, chest and pelvic accelerations, and neck forces. Some dummies also had instrumentation in the upper and lower legs to measure the forces caused by contact with the seat in front of the dummy.

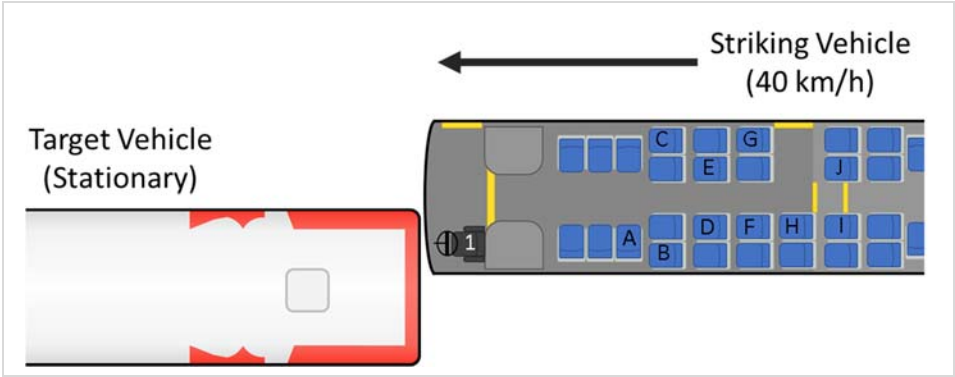

Legend Test 1 and Test 2	
1	Hybrid III 50th percentile
A	WorldSID
B, J	Hybrid III ten-year-old
C, G	Hybrid III six-year-old
D, E, F, I	Hybrid III 5th percentile
H	Hybrid III 50th percentile

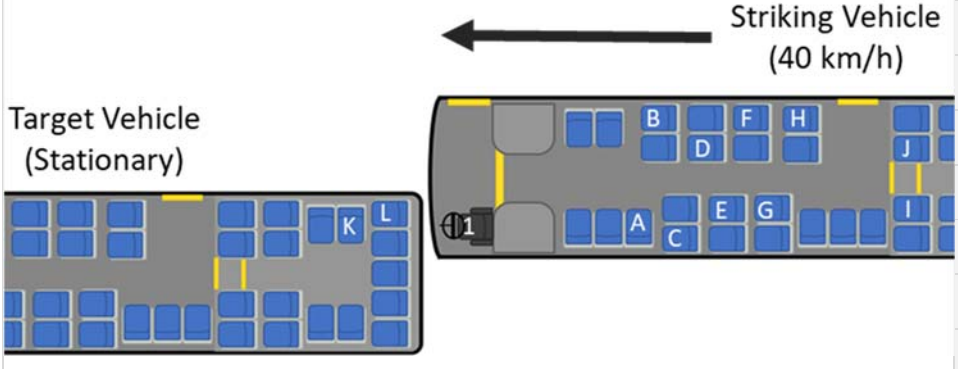

Legend Test 3 and Test 4	
1	Hybrid III 50th percentile
A	WorldSID 50th percentile
C, J	Hybrid III ten-year-old
B, F, H	Hybrid III six-year-old
D, E, G, I	Hybrid III 5th percentile
K	WorldSID 5th percentile
L	Hybrid III 50th percentile

Figure 3: Schematic of the crash test dummy placement on-board the vehicles for Test 1 & Test 2 and Test 3 & Test 4.

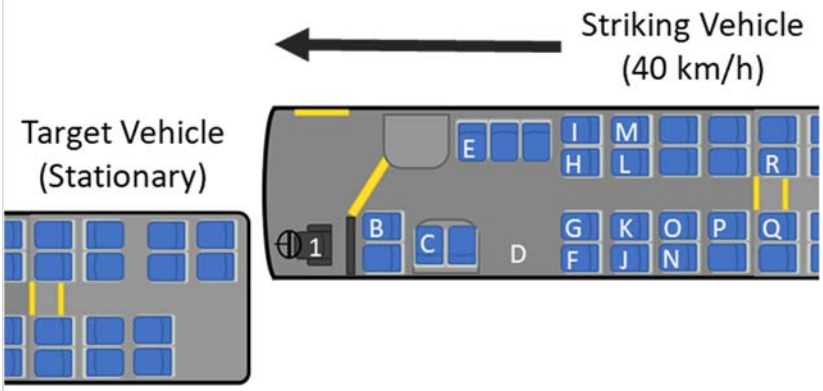

Legend	
1, Q	Hybrid III 50th percentile
D	Hybrid III 50th percentile in a wheelchair facing forward
J, K, P, R	Hybrid III 5th percentile
O	THOR 5th percentile
C, E	WorldSID 5th percentile
B, I	Hybrid III 10-year-old
H	Q-Series 10-year-old
F, M, N	Hybrid III 6-year-old
G, L	Q-Series 6-year-old

Figure 4: Schematic of the crash test dummy placement on-board the Striking Vehicle for Test 5.

3.2 RESULTS

3.2.1 Visual Records of Bus Deformation

3.2.1.1 Test 1, Test 2, Test 3 and Test 4

Post crash photos of the front left corner of the bus for Test 1 and Test 2 and Test 3 and Test 4 are presented in Figure 5 and observations are summarized in Table 1. For both target vehicles, beneath the service panel, there was significant deformation and displaced non-structural components. The members that support the A-pillar were significantly deformed. At the base, the A-pillar sheared completely and was displaced into the body. The upper section of the A-pillar, adjacent to the window, was disrupted at the midpoint in Test 1 but not Test 3. On the driver side, the bumper was folded back and into the space previously occupied by the base of the A-pillar. Little to no deformation was found on the underbody structure of Test 1, 2 and 3. The photos in the right panels of Figure 5, suggest that the reinforcements of the Striking Vehicle for Test 2 and Test 4 appear to have limited deformation at the front of the bus and the driver occupant space.

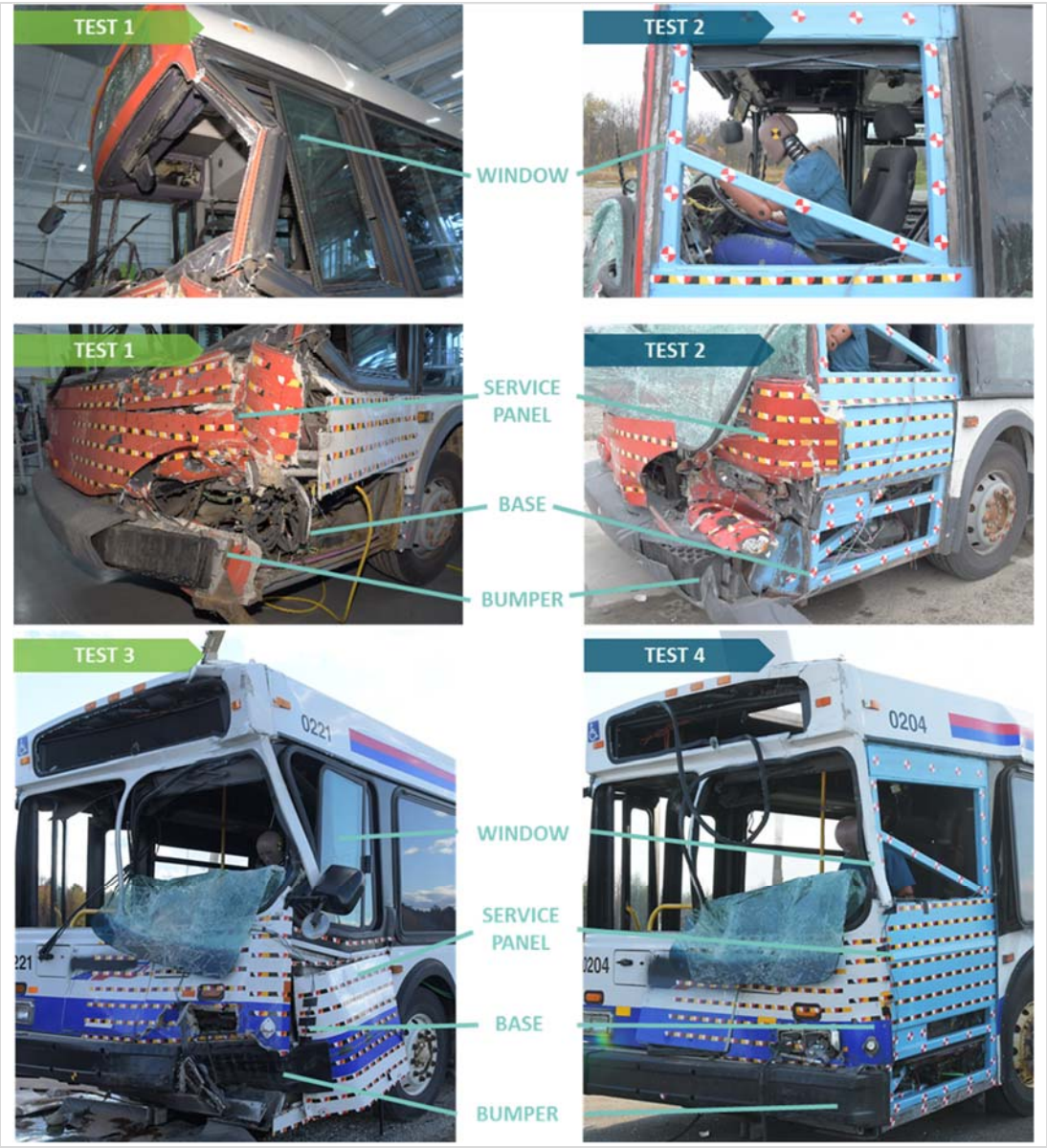

Figure 5: Post test photos of the Striking Vehicle in Test 1, Test 2, Test 3 and Test 4.

Table 1: Summary of damage observed in Test 1, Test 2, Test 3 and Test 4.

Bus Location	Test 1 Observation	Test 2 Observation	Test 3 Observation	Test 4 Observation
Bumper support beam	Visibly bent	Deformation not visually obvious	Visibly bent	Deformation not visually obvious
Base	A-pillar disruption	No apparent A-pillar disruption	A-pillar disruption	No apparent A-pillar disruption
Window	A-pillar bent	A-pillar not visibly bent	A-pillar bent	A-pillar not visibly bent
Service panel	Deformation	Slight deformation	Deformation	Slight deformation
Underbody	No apparent deformation observed			Significant skew

3.2.1.2 Test 5

The resulting damage to the striking vehicle can be seen in Figure 6. The A-pillar/windshield frame of the striking bus was displaced rearward into the occupant compartment. The front body panel of the bus was also displaced rearward, along with the bumper. The bumper was deformed primarily where it met with the right edge of the target bus. No major rearward displacement was visually observed along the side of the bus or underneath the front. The frame surrounding the driver's sliding window does not appear to be displaced.

Figure 6: Post test photo of Striking Vehicle in Test 5.

3.2.2 Recorded Displacements of Marked Locations

3.2.2.1 Test 1, Test 2, Test 3 and Test 4

The 3D locations of targets, placed in identical locations on the fronts of the buses, were recorded pre- and post-crash. Results are shown in Figure 7. The longitudinal displacements were used as indicators of intrusion. The maximum displacement on the bottom half of the bus was reduced from 366 mm in Test 1 to 260 mm in Test 2. At the A-pillar near the window frame, the displacement was reduced from 261 mm in Test 1 to 22 mm in Test 2.

Targets for Test 3 and Test 4 were also placed in identical locations however, but were limited to structural components to facilitate analysis. The maximum displacement on the bottom half of the bus was reduced from 457 mm in Test 3 to 207 mm in Test 4. At the A-pillar near the window frame, the displacement was reduced from 273 mm in Test 3 to 80 mm in Test 4. The 3D location data confirms that the reinforced section in Test 4 experienced a significant pitch rotation and slight outward rotation. The A-pillar targets are mostly collinear but have been shifted back and pitched down as a whole, relative to the pre-test measurements. The topmost point of the A-pillar is 28 mm rearward of the pretest location while the bottommost point of the A-pillar has shift back 166 mm and down 78 mm.

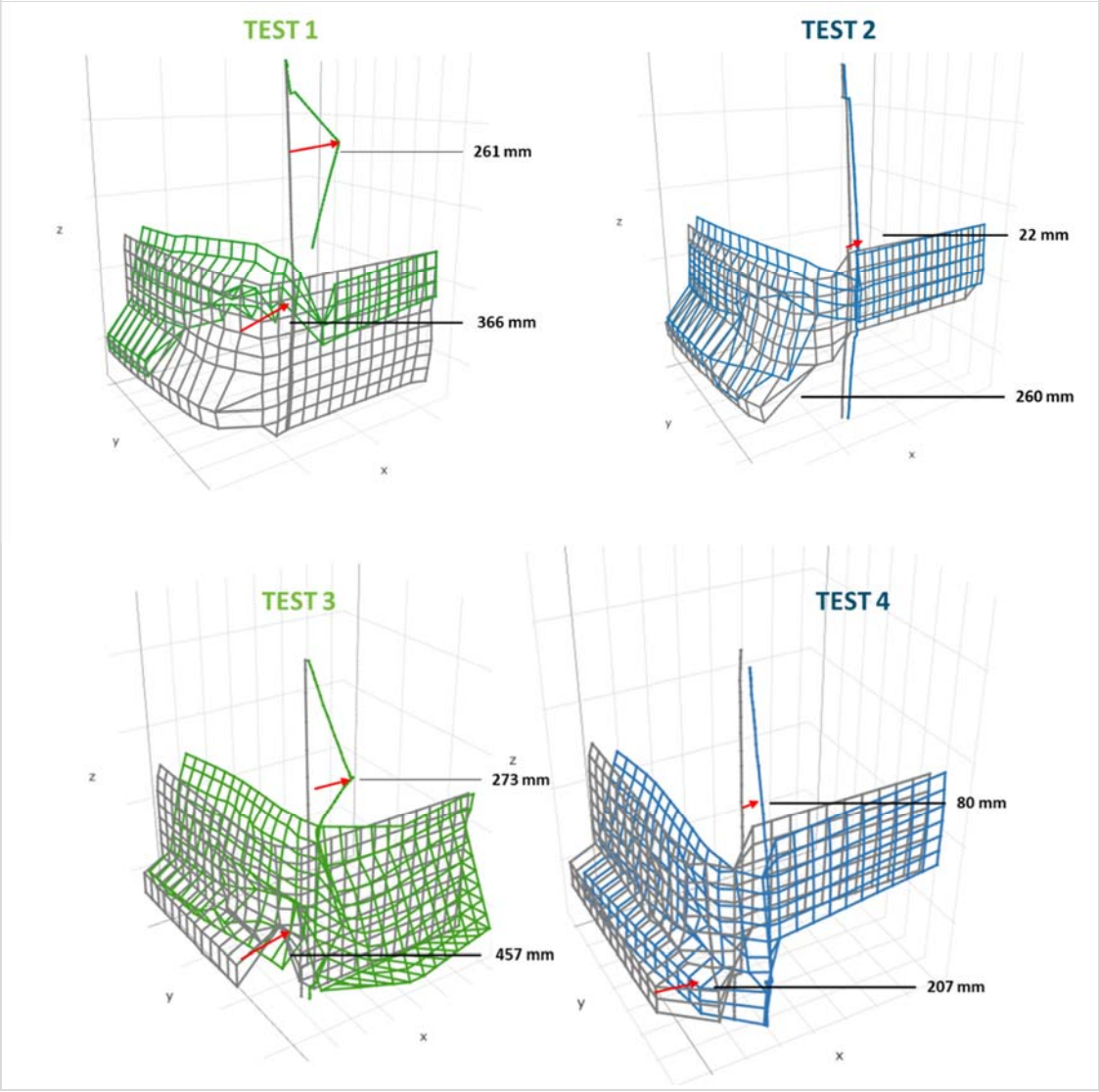

Figure 7: Overlays of the 3D locations of targets on the front of the bus, recorded pre-test (grey) and post-test, green for Test 1 and Test 3, blue for Test 2 and Test 4.

The displacement of the underbody in both Test 3 and Test 4 was quantified with 3D point streams along the underside of the front of the bus. The point streams were recorded along the most prominent structural members pre-test and post-test. As shown in Figure 8, the streams confirm that the underbody of the bus in Test 4 was displaced. The top-down projection shows the yaw and rearward displacement of the front of the bus. The downward pitch measured 53 mm at its greatest on the leftmost beam and 27 mm on the rightmost beam. The yaw to the left was 74 mm on the leftmost beam.

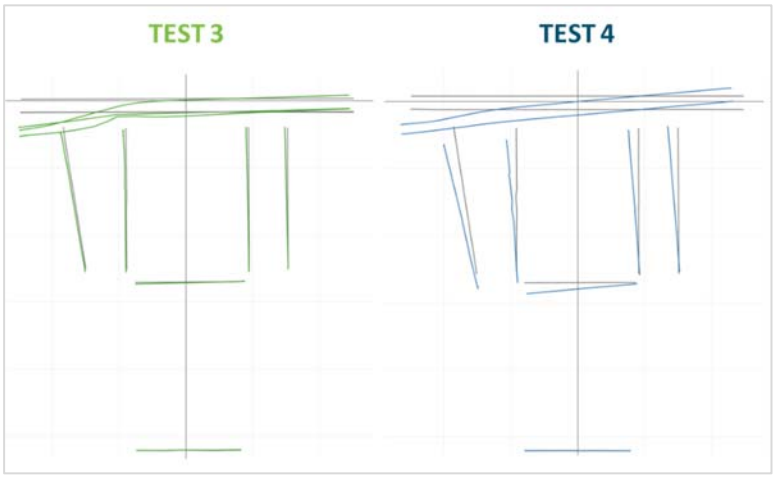

Figure 8: Overlays of the 3D locations of point streams of the underbody of each bus (in the X-Y plane, top-down view), recorded pre-test (grey) and post-test (green for Test 3, blue for Test 4).

3.2.2.2 Test 5

The 3D locations of targets placed along the front below the windshield, on the side below the driver window, and along the A-Pillar were recorded pre- and post-crash for Test 5. Overlays of the pre-test and post-test measurements in Test 5 are presented in Figure 9.

The longitudinal displacements were used as indicators of intrusion. At the A-pillar near the window frame, the displacement was measured at 290 mm. At the base of the A-Pillar, 226 mm. The broken body panels revealed a steel column at the front edge of the frame of driver's sliding window. When compared to the body panel covering it pre-test, there did not appear to be any deformation of this structure. The displacement of the actual body panel itself was primarily lateral, in the longitudinal direction it was no more than 7 mm along the top half. The greatest longitudinal displacement along the front of the bus was 313 mm, located 400 mm to the left of center and just below the windshield.

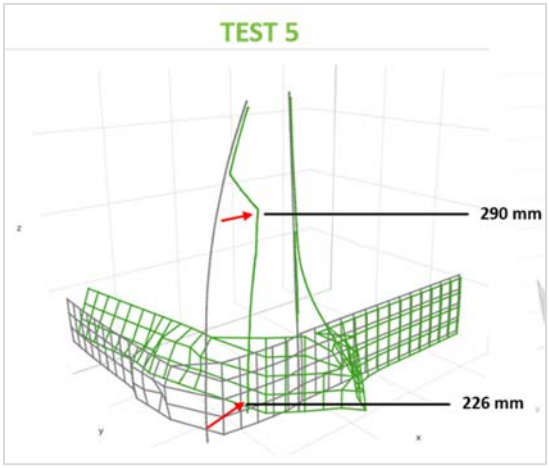

Figure 9: Overlays of the 3D locations of targets on the front of the bus, recorded pre-test (grey) and post-test (green) in Test 5.

The displacement of the underbody was quantified with 3D point streams along the underside of the front of the bus. The point streams were recorded along the most prominent structural members pre-test and post-test. As shown in Figure 10, the streams confirm that the underbody of the bus in Test 5 was not significant deformed or displaced. There is however a slight downward pitch movement of 20-35 mm. On the struck side, there is deformation of the lateral beam supporting the bumper and the longitudinal beam on the left side to which meets with it – 65 mm vertically and 50 mm longitudinally.

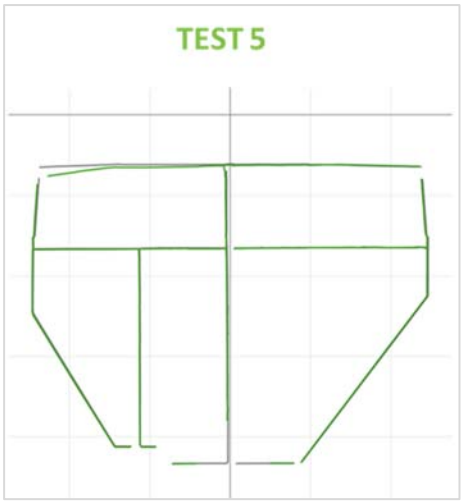

Figure 10: Overlays of the 3D locations of point streams of the underbody of the bus (in the X-Y plane, top-down view), recorded pre-test (grey) and post-test (green).

3.2.3 Accelerations Responses of the Bus

3.2.3.1 Test 1, Test 2, Test 3, Test 4

Placement of the accelerometers on the two striking buses for Test 1 and Test 2 were matched. Fore-aft acceleration responses were significantly lower than the values typically observed in light duty vehicles tested in comparable crash test configurations. As shown in Figure 11, all peak fore-aft acceleration responses of the Striking Vehicle were slightly greater in Test 2 than in Test 1. The greatest peak acceleration recorded in Test 1 was 7.0 g compared to 9.7 g in Test 2. There was no obvious relationship between the individual accelerometer locations and the region of impact.

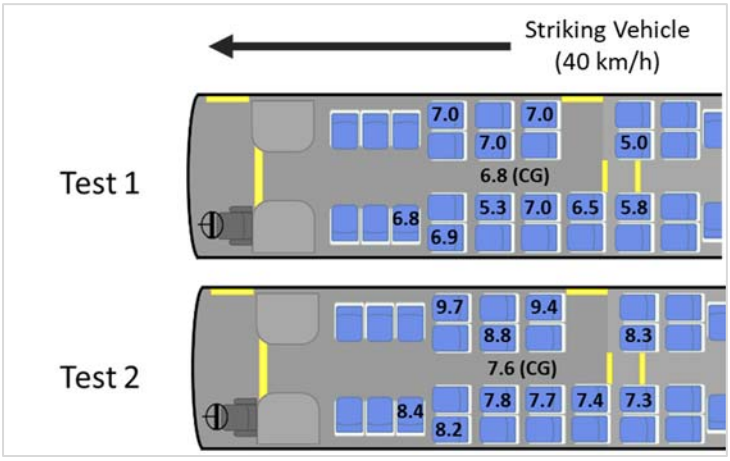

Figure 11: Peak fore-aft acceleration responses as a function of location in Test 1 and Test 2.

Placement of the accelerometers on the two striking buses for Test 3 and Test 4 was matched. As shown in Figure 12, all peak fore-aft acceleration responses of the Striking Vehicle were slightly reduced in Test 4 compared to Test 3, averaging an 8.8% decrease in peak acceleration. The accelerations at the driver locations could not be included in the analysis due to excessive noise.

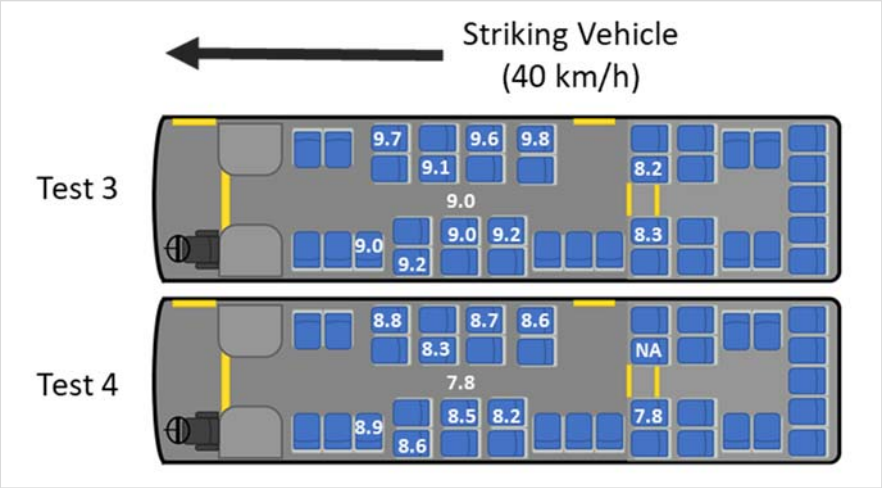

Figure 12: Peak fore-aft acceleration responses in the striking vehicle as a function of location in Test 3 and Test 4.

The velocity profiles at each seat, derived from integrating each acceleration-time trace, are also very similar. The average total change in velocity at each seat was only 4.1% higher in Test 4 when compared to Test 3. In contrast, between Test 1 and 2, there was a 23.9% increase in peak acceleration and a 7.9% increase in measured change in velocity in Test 2. The velocity profiles in Test 2 also indicate that the minimum velocity was reached sooner than in Test 1, at all measured locations, by 40 ms on average. There was no significant difference in time to minimum velocity in Test 4 compared to Test 3, which was 4 ms sooner on average. Figure 13 presents the peak fore-aft acceleration responses of the Target Vehicle:

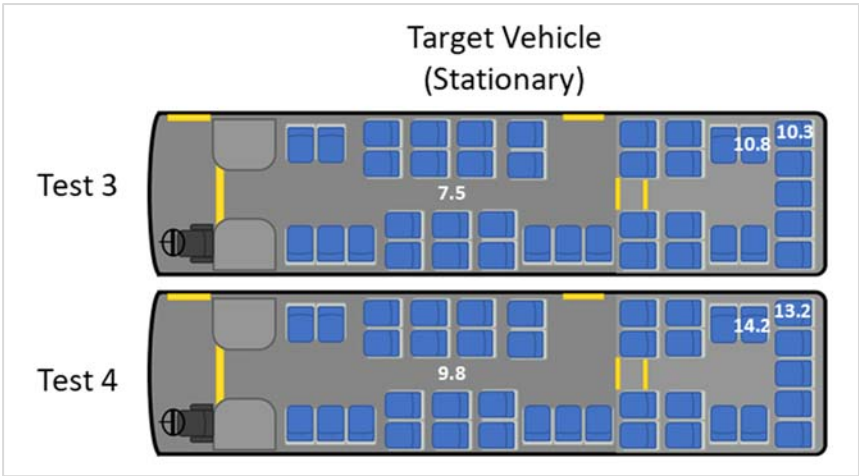

Figure 13: Peak fore-aft acceleration responses in the Target Vehicle as a function of location in Test 3 and Test 4.

In the Target Vehicle, all peak fore-aft acceleration responses increased in Test 4, averaging a 30.3% increase. The velocity profiles from each accelerometer are again very similar, the total change in velocity measured averaged only 2.9% higher in Test 4 compared to Test 3. The lack of increase in peak fore-aft acceleration and change in velocity indicates that the structure of the B40LF bus did not respond in the same way as the D40i bus used in the first series of tests, whose peak fore-aft accelerations and change in velocity both increased. This suggests that the energy transfer is different, possibly that the energy absorption is occurring at the front of the bus but not by the reinforced section.

In Test 4, it appears that the deformation was relocated to the structures surrounding the wheel well. The front of the bus appears to have pitched, shifted, and yawed as a whole. Unlike Test 1, Test 2 and Test 3, deformation of the underbody of the bus was pronounced.

Combining visual observations of deformation, 3D point streams, and accelerometer data, it appears that the energy of the impact was absorbed in large part through the structures surrounding the wheel. There was deformation evident at the front of the bus, in the wheel housing, the floor adjacent to the wheel housing, and window frame above the wheel. No visible deformation was evident further down the bus. High-speed video of the collision shows that the wheel itself was compressed during the impact event when the wheel housing began deforming. A large amount of plastic and elastic deformation in this area has potential to absorb much of the collision energy. This explains why, in contrast to Tests 1 and 2, the peak fore-aft accelerations did not increase and even reduced slightly. Although the reinforced front end of the bus was displaced during the collision, the collision energy was not transferred as readily to the passenger section of the bus as in Test 2.

3.2.3.2 Test 5

The peak acceleration at the center of the target bus was 7.1 g, while the peak at the center of the striking bus was 8.5 g. The accelerations at each place in the striking bus (Figure 14) ranged from 8.0 to 16.9 g, tending higher at the front of the bus.

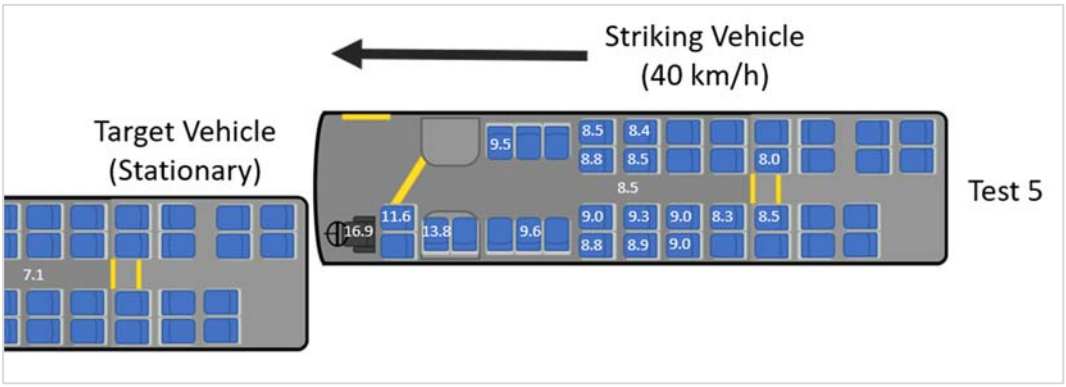

Figure 14: Peak fore-aft acceleration responses in the target and striking vehicles as a function of location, in Test 5.

The velocity profiles at each seat, derived from integrating each acceleration-time trace, are also very similar. There does not appear to be much relative velocity between the accelerometers, suggesting that the bus structure did not deform or decelerate much more in some places than in others. The difference in peak acceleration appears to be primarily due to varying amplitudes of oscillation in the signal.

The structures at the rear of the target bus are also different on the LFS 40102. There are fewer strong structural elements along the floor of the bus. Notably, it lacks the large frame rails in the middle third of the bus that are present in the B40LF, which support the engine. The LFS's engine is mounted on the left – non-struck – side of the bus. Visually, greater deformation was observed at the rear of the target vehicle in Test 5 than in any of the previous tests. The rear bumper was displaced further into the bus. The underbody dropped down from the struck side, it detached all the way to the rear wheel arch. The relative rigidities at the front and at the rear of the buses affects the transfer of energy between them in a collision.

3.2.4 Dummy Responses

3.2.4.1 Test 1, Test 2

Results are presented for Test 1 and Test 2, then Test 3 and Test 4, and finally for Test 5. The analysis was carried out by combining the visual and contextual information provided by high-speed videos with the quantitative data recorded by dummy instrumentation. Responses for each test series are grouped by dummy location and stature; where multiple dummies shared similar characteristic motions, the response of a representative dummy is provided.

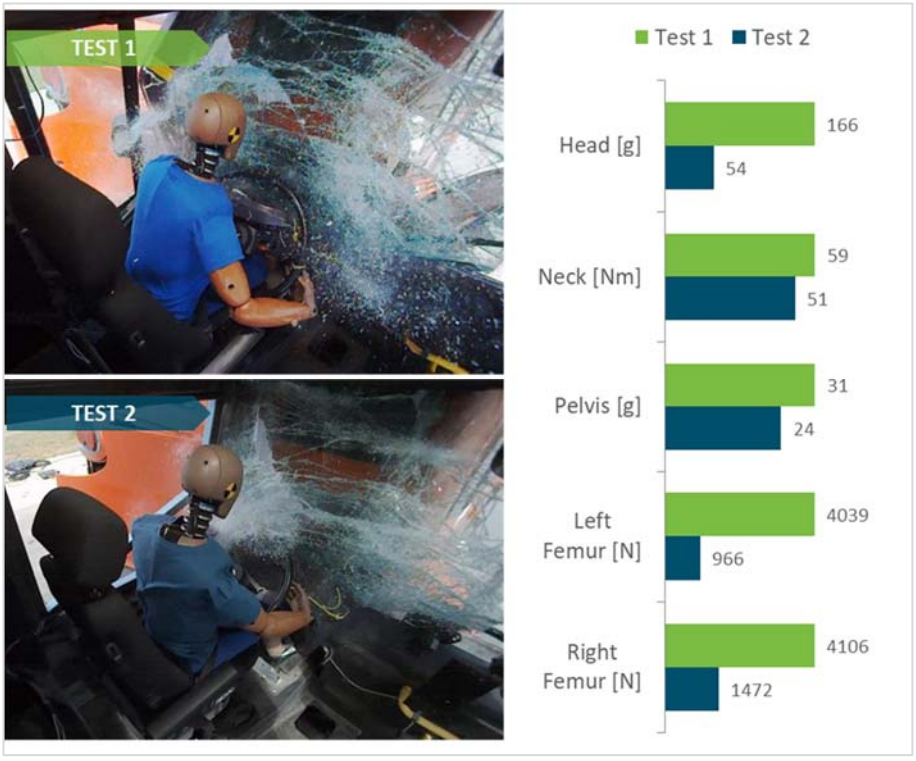

Figure 15: Freeze frames of the driver dummy at peak head excursion Tests 1 and 2 (left panel) and the peak head, neck, pelvis and femur responses (right panel)[1].

[1] Bar charts have been normalized for presentation purposes.

Figure 15 presents two freeze frame images comparing the interaction of the driver with the intruding structure. The disrupted A-pillar in Test 1 can be seen just above and to the left of the driver head in the top image. In comparison, the A-pillar for Test 2, seen in the lower image, appears intact. In both tests, the head appeared to have contacted the windshield, and the steering wheel and instrument panel were displaced rearward into the body of the driver dummy.

Head, neck, pelvis, and femur responses of the driver dummy were all lower in Test 2 than in Test 1, with the greatest reductions occurring at the head and femurs. The head acceleration was reduced from 166 g in Test 1 to 54 g in Test 2, a reduction of 67 %, suggesting that there was a significant head impact in Test 1 and no impact in Test 2. Indeed, the video indicates that the dummy head contacted the rear leading edge of the target bus in Test 1 but not in Test 2. Left and right femur loads in Test 2 were reduced by 76 % and 64 % of the respective loads recorded in Test 1. Note that the chest deflection responses, while recorded for both tests are not presented in the plot.

In the lateral views of the videos for Test 1, the dummy pelvis was displaced rearward by the intruding structures. The extent of the intrusion and the concurrent rearward displacement were not observed for Test 2. Post-test photos of the driver in Figure 16 illustrate the difference in the final position of the dummy relative to the steering wheel and instrument panel. In Test 1 (upper left photo), there is no gap between the pelvis and the seat back and the knee joint is on the seat cushion, whereas in Test 2 (upper right photo), there is a visible gap between the pelvis and the seat back, and the knee joint is forward of the seat cushion. In the post-test close-up views of Test 1 (lower left photo), the steering wheel is wedged into the space between the rib cage and the dummy abdomen while in Test 2 (lower right photo), only the shirt of the dummy is in contact with the steering wheel. As noted previously, there are no sensors in this region of the dummy to quantify the loading.

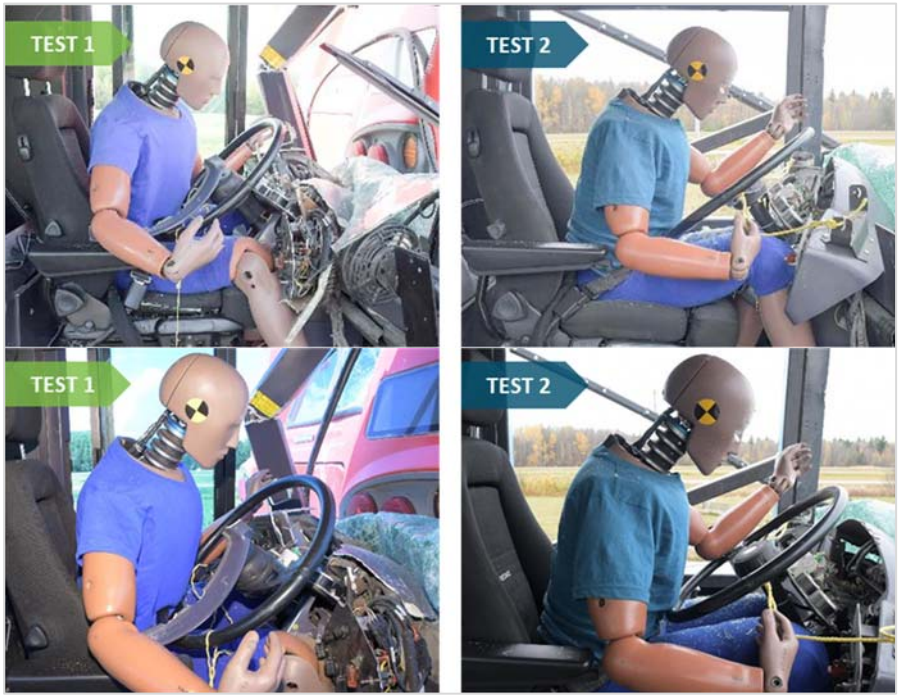

Figure 16: Final position of dummy in the driver seat following Test 1 (left) and Test 2 (right).

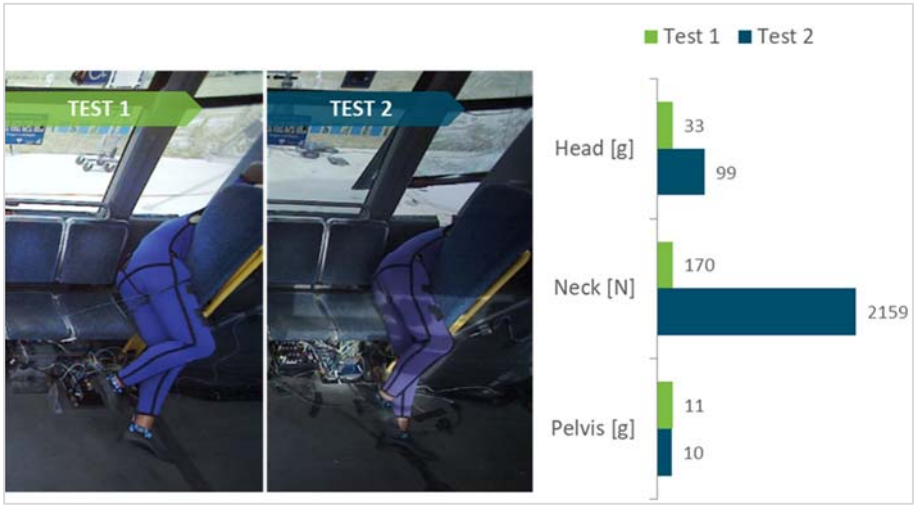

Figure 17: Freeze frames at peak head excursion for the dummy seated in Position A in Tests 1 and 2 (left panel) and the peak head, neck, and pelvis responses (right panel).

Figure 17 presents a freeze frame image of the WorldSID 50th side impact dummy at the moment of peak head excursion for Test 1 and Test 2. In both tests, the dummy was displaced vertically and projected in an upright seated posture towards the front of the bus until the motion of the pelvis and upper legs were stopped by the upholstered barrier. The upper body continued to move towards the front of the bus in the space between the upholstered barrier and the window. In Test 1, the upper body did not extend as far forward as in Test 2, and the torso of the dummy rebounded out of the space. In Test 2, the head extended further forward, impacted a rigid panel located behind the driver seat, and remained trapped between the barrier and the window. The dummy head and neck responses confirmed that the impact of the head was more severe in Test 2.

The head impact for the side-facing dummy in Test 1 resulted in a peak head acceleration of 33 g compared to 99 g in Test 2; the upper neck shear increased from 170 N in Test 1 to 2 159 N in Test 2. Pelvis accelerations were similar in both tests. Shoulder and rib responses were recorded, but the sensors are not aligned to measure this type of loading. The side impact dummy was designed to measure a perpendicular side impact load directed towards the shoulder, side of the chest, and pelvis.

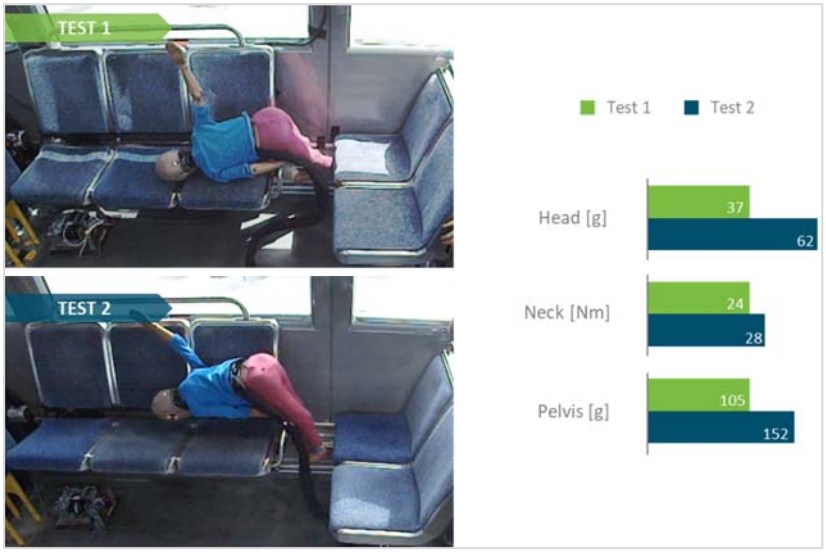

Figure 18: Freeze frames at peak head excursion of the 6-year-old dummy in Position C in Tests 1 and 2 (left panel) and the peak head, neck, and pelvis responses (right panel).

The movement of the child dummies placed in the first rows (Position B & C) were comparable for Test 1 and Test 2. In both tests, the child dummies were ejected out of the seats they occupied. In each test, the motion of the lower body was interrupted by the side-facing seat located in front of the dummy as the upper body pivoted forward, over the side bench armrest. As shown in the freeze frame images for Position C in Figure 18, the heads contacted slightly different locations on the side-facing seats and the orientation of the torso was different. In both tests, the dummy in Position C remained on the side-facing seats. The ten-year-old dummy that was seated in Position B, rolled off the side-facing seat, onto the floor in both tests.

To the right of the images in Figure 18 are the corresponding head, lower neck, and pelvis responses of the 6-year-old dummy in the first-row for the two tests. The head, lower neck, and pelvis responses of this dummy in Test 2 were 67 %, 16 %, and 45 % greater than each respective response in Test 1.

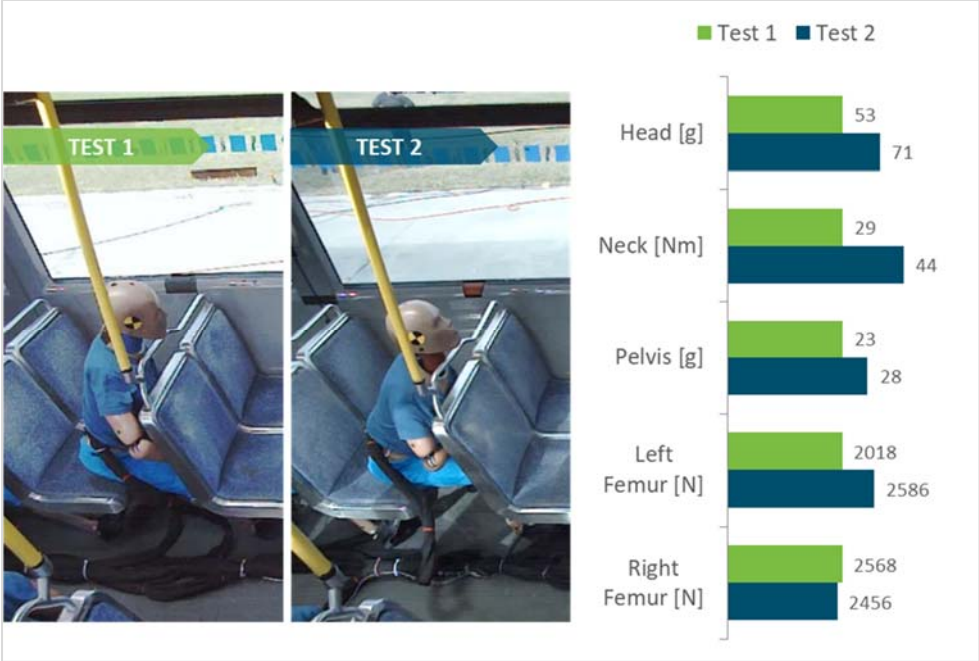

Figure 19: Freeze frames at peak head excursion of the 5th percentile dummy in Position D in Tests 1 and 2 (left panel) and the peak head, neck, pelvis, and femur responses (right panel).

As a representative example of the 5th percentile dummy responses in the mid rows, Figure 19 presents the freeze frame images and kinematic and kinetic responses of the 5th percentile dummy in the 2nd row (Position D). In Test 1 and Test 2, the dummies in locations D, E and F translated forward until the knees struck the lower seat back of the seat in front. The upper body then pivoted forward until the chin impacted the handrail on top of the seat in front. In Test 1 and Test 2, the chin remained in contact with the handrail, and the head-neck complex extended rearward as head translated upwards. In both tests and all locations, the 5th percentile head contacted the hand rail. In the representative example (Figure 19), the responses of the dummy in Position D were greater in Test 2 than in Test 1 at the head, neck, pelvis, and left femur. The greatest percentage increase occurred at the neck: the bending moment in Test 2 was 48 % greater than the moment in Test 1. The left femur load was greater in Test 2 while the right femur responses were comparable for Test 1 and Test 2.

The 50th percentile dummy placed in the fourth row (Location H) also contacted the seat in front with the knees and the upper body flexed forward. In Test 1, the 50th percentile dummy contacted the handrail at the neck. In Test 2 the chin contacted the handrail. For this dummy, differences in the initial pre-test positions between the two tests were identified and may have led to the observed differences in motion. The neck is instrumented with force transducers at the top and base of the neck; therefore, contact in the centre of the neck, particularly at low energy levels, may not be adequately detected.

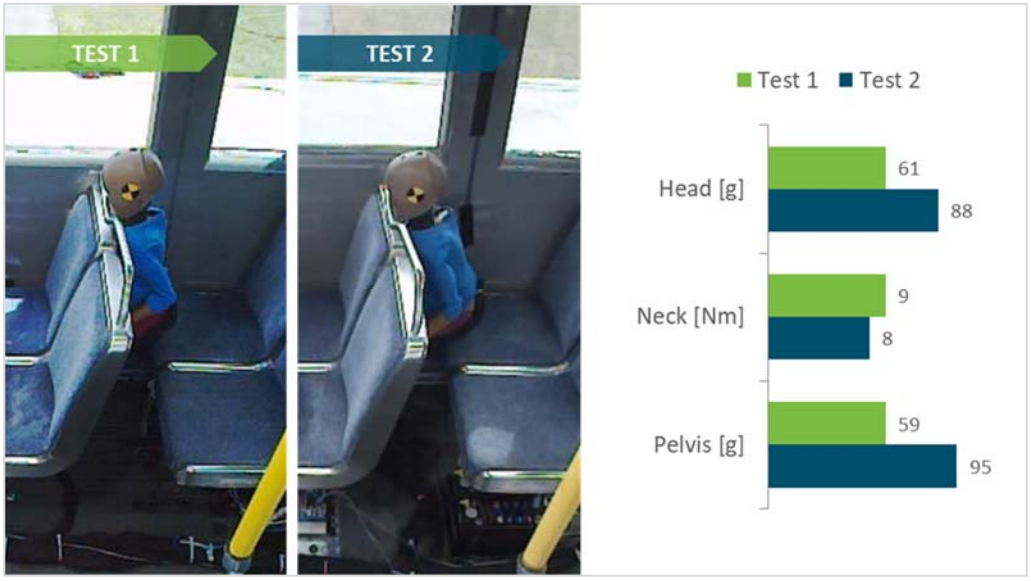

Figure 20: Freeze frames at peak head excursion of the 6-year-old dummy in Position G in Tests 1 and 2 (left panel) and the peak head, neck, and pelvis responses (right panel).

In Test 1 and Test 2 the child-sized dummy in the mid rows (Position G), contacted the seat in front of it with its head, torso, and legs. Figure 20 presents the freeze frame images and corresponding kinematic and kinetic responses of the six-year-old dummy in the 3rd row (Position G). The dummy experienced greater head, neck, and pelvis responses in Test 2 than in Test 1, with percentage increases of 45 %, 24 %, and 60 %, respectively.

The dummies were sometimes found in positions that were not at all representative of what would be expected of a human child. Figure 21 presents the post-test images for the child sized dummy in position G following Tests 1 and 2.

Figure 21: Post-test photos illustrating postures of the six-year-old Hybrid III dummy in Position G.

Figure 22: Freeze frames at peak head excursion of the 5th percentile dummy in Position I in Tests 1 and 2 (left panel) and the peak head, neck, pelvis, and femur responses (right panel).

Both dummies seated on the second level of the bus traveled forward, contacted the barriers in front of them, and pivoted over the barrier. The images in Figure 22 suggest that the dummy rotated further over the barrier in Test 2, as evidenced by the position of the head, height of the pelvis, and extension of the legs. The representative responses shown in Figure 22 are those of the 5th percentile dummy (Position I). The head, neck, pelvis, and femur responses in Test 2 were between 6 % and 89 % greater in magnitude than the corresponding responses in Test 1.

3.2.4.2 Test 3 and Test 4

Figure 23: Freeze frames at 95 ms of the dummy in the driver location for Tests 3 and 4 (left panel) and the peak head, neck, pelvis, and femur responses (right panel).

Figure 23 presents freeze-frame images of the 50th percentile dummy at 95 ms, just before the view is obstructed by glass shards, peak responses for the driver in Test 3 and Test 4 are shown in the panel to the right. The dummy was restrained only by the lap belt. The head and torso rotated forward as the dummy translated forward in the seat. In both tests, the instrument panel and steering wheel were displaced into the driver space but there was no impact with the dummy head. This is corroborated by the peak accelerations of the head which were 23 g and 25 g in Test 3 and 4, respectively. In Test 3, the lower rim of the steering wheel loaded the dummy at the sternum contributing to a peak chest deflection of 46 mm. In Test 4, however, the lower rim of the steering wheel loaded the abdomen well below the instrumentation of the thorax resulting in a peak chest deflection of only 6 mm.

The peak left and right femur loads were 3674 N and 6821 N in Test 3 and 2954 N and 3336 N, respectively in Test 4. The right femur value of 6821 N was of extremely short duration and was not detected when the sampling rate was reduced from 20k to 10k.

There were 10 dummies of different sizes and type placed in passenger seats. In both Test 3 and Test 4 the heads of all five dummies that were placed in the middle section of the bus, struck the handrail of the seat immediately in front; the other five were either partially ejected from the seat and found suspended over barriers or completely ejected from the seat and found on the floor.

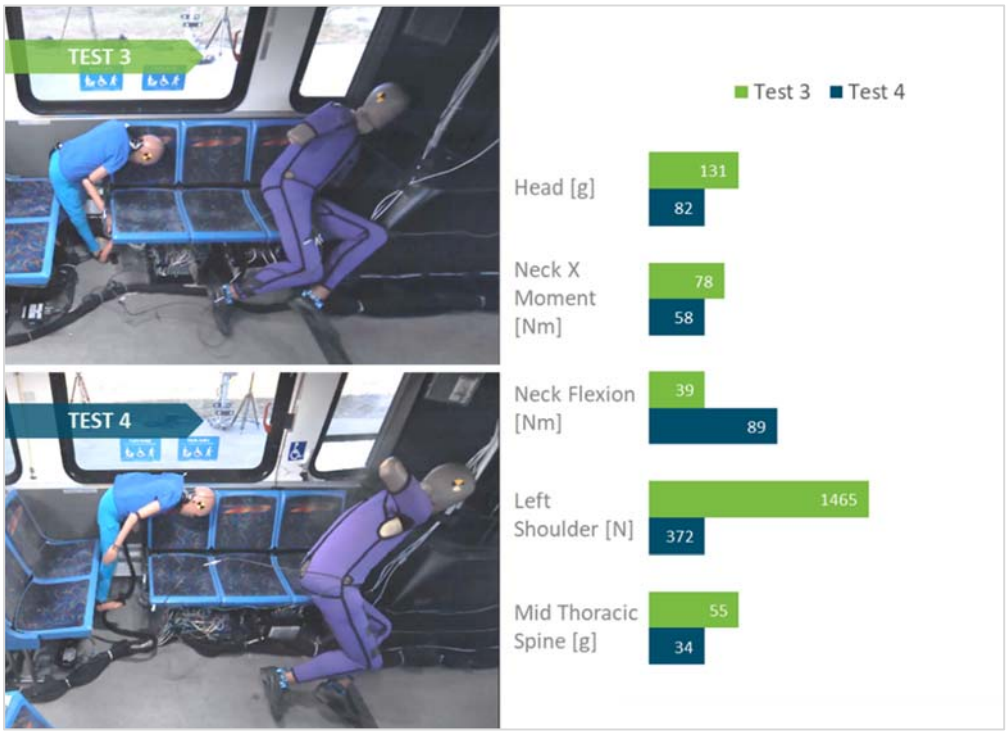

Figure 24: Freeze frame images of the dummy in Position A in Tests 3 and 4 (left panel) and the peak head, neck, shoulder, and spine responses (right panel).

Figure 24 presents freeze-frames of the side-facing 50th percentile side impact dummy seated at position A at the moment of head contact with the adjacent surfaces of the bus for Test 3 and Test 4. In both tests, the dummy was initially projected in an upright seated posture towards the front of the bus. In Test 3, at approximately 260 ms the dummy head strikes the wheel housing and route information panel resulting in a peak head acceleration of 131 g, the dummy was not ejected from the seat. In Test 4, the dummy head strikes the vertical hand rail at 280 ms and was ejected from the seat, into the aisle between the driver and the front doors.

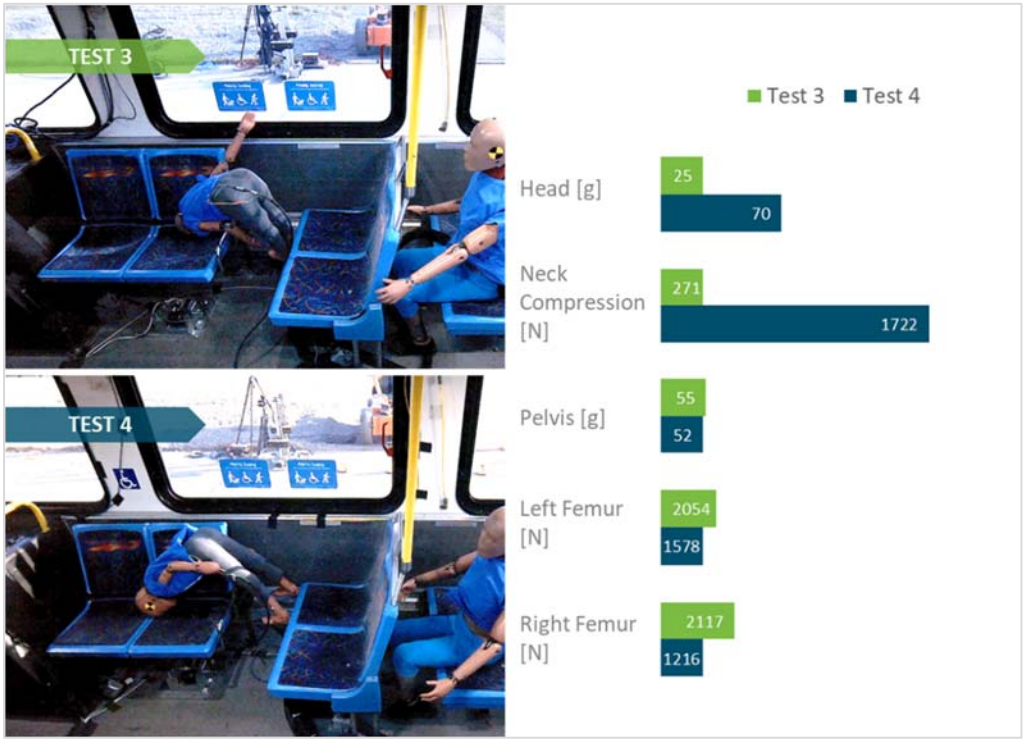

Figure 25: Freeze frames at the time of head contact (left panel) of the dummy seated in Position B in Tests 3 and 4 and the peak head, neck, pelvis, and femur responses (right panel).

Figure 25 presents freeze-frames and responses for the Hybrid III 6-year-old dummy seated in Position B (non-struck side of the bus). In both tests the dummy translated forward until the knees struck the edge of the side-facing seat. In Test 3 and Test 4 the dummy was pitched over the arm rest of the side-facing seat. In Test 3 the trajectory of the dummy was interrupted by the interaction between the dummy pelvis and the arm rest, and the dummy was eventually ejected from the seat into the aisle. In Test 4, the dummy pelvis cleared the arm rest of the side-facing seat, the head impacted the separation between the side-facing seats and remained in the position shown in the bottom freeze frame of Figure 25. The peak head acceleration for this dummy was 70 g and the peak neck compression was of the order of 1700 N.

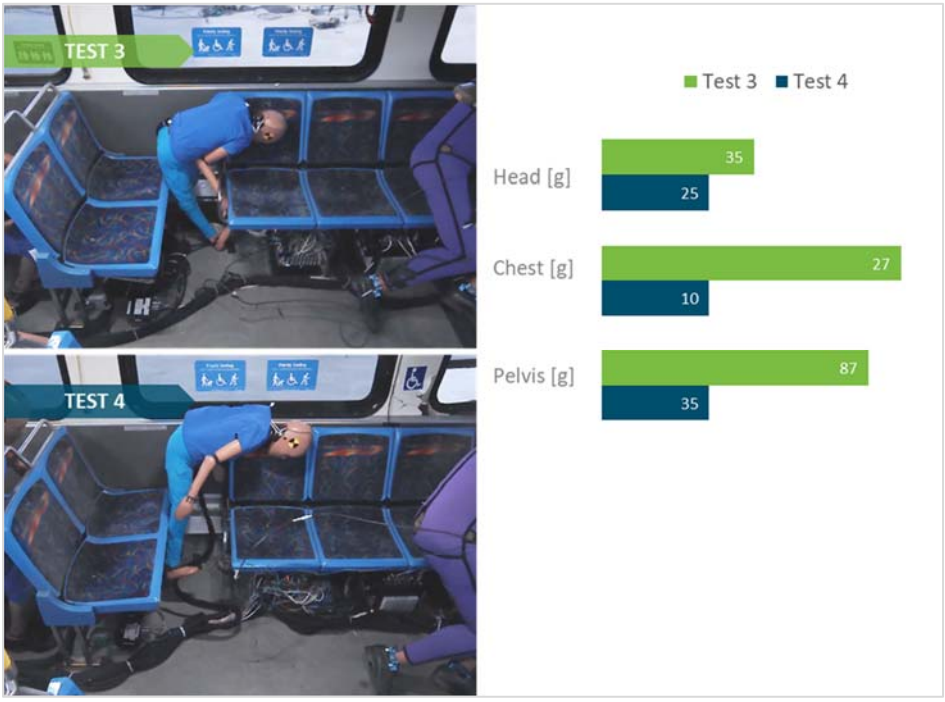

Figure 26: Freeze frames of the dummy seated in Position C in Tests 3 and 4 (left panel) and the peak head, chest, and pelvis responses (right panel).

Figure 27: Photo of final position in Test 3.

Figure 26 a presents freeze-frames and responses for the Hybrid III 10-year-old dummy seated in Position C. In both tests the dummy translated forward until the right knee impacted the arm rest of the side-facing seat and the left knee struck the edge of the side-facing seat. In Test 3, interaction of the right hand and arm with the side-facing seat altered the trajectory of the dummy and prevented ejection from the seat. Figure 27 is a post test photo showing the right hand of the dummy wedged in the space between the seat edge and the arm rest. In Test 4, the right knee impacted the arm rest while the left knee struck the edge of the side-facing seat back, the dummy then rotated over the arm rest coming to rest with the pelvis on the arm rest.

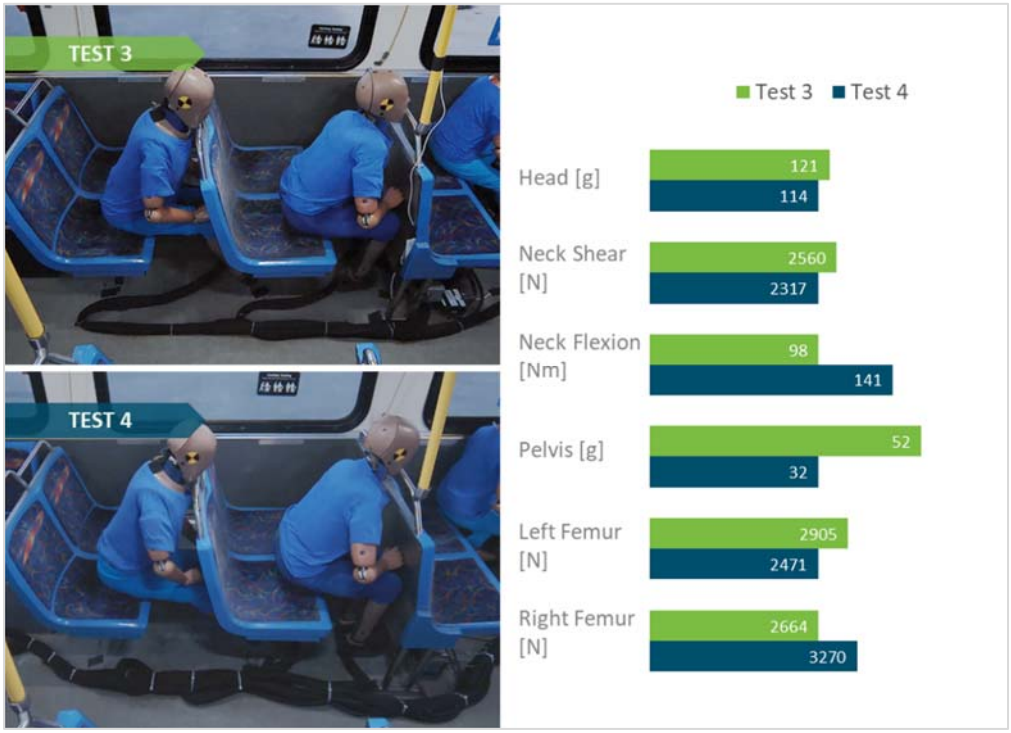

Figure 28: Freeze frames of the dummy seated in Position E and G (left) for Tests 3 and 4 (left panel) and the peak head, neck, pelvis, and femur responses for position E (right panel).

Figure 28 presents freeze-frames of the 5th percentile dummy positioned in E (row 2, left side of bus) and in G (row 3, left side of bus) for Test 3 and Test 4. In Test 3 the dummies located in positions E and G, translated forward until the knees struck the seatback of the seat directly in front. At the time of knee impact, the legs of the dummy seated in E were flexed with the feet immediately below the lower legs, the head and torso then pivoted forward until the face of the dummy collided with the handrail atop the seat in front. In position G (immediately behind E), the feet extended further forward, below the seat in front. The pelvis translated upwards causing the head and neck to be displaced upwards above the handrail, eventually coming to rest with the neck on the hand rail. The motion of the dummy seated in position D, across the aisle was comparable to the dummy in position E.

In Test 4 the dummies located in positions E and G, translated forward until the knees struck the seatback of the seat directly in front however, the dummy in position E exhibited much greater vertical lift and came to rest with the neck on the hand rail.

Figure 29: Freeze frames of the dummies seated in Position F and H for Tests 3 and 4 at the time of peak head/neck response (left panel) and the peak head, neck, and pelvis responses for Position F (right panel).

Figure 29 presents freeze-frames of the Hybrid III 6-year-old seated in Position F and H on the non-struck side of the bus. In Test 3 and Test 4 both dummies translated forward and both heads impacted the hand rail. The dummy seated in F slid into the space between the seats and remained in a suspended and upright seated posture as shown in Figure 30. The dummy seated in H rebounded back in the seat.

Figure 30: Photos of post test position for the dummy seated in location F for Test 3 (left) and Test 4 (right).

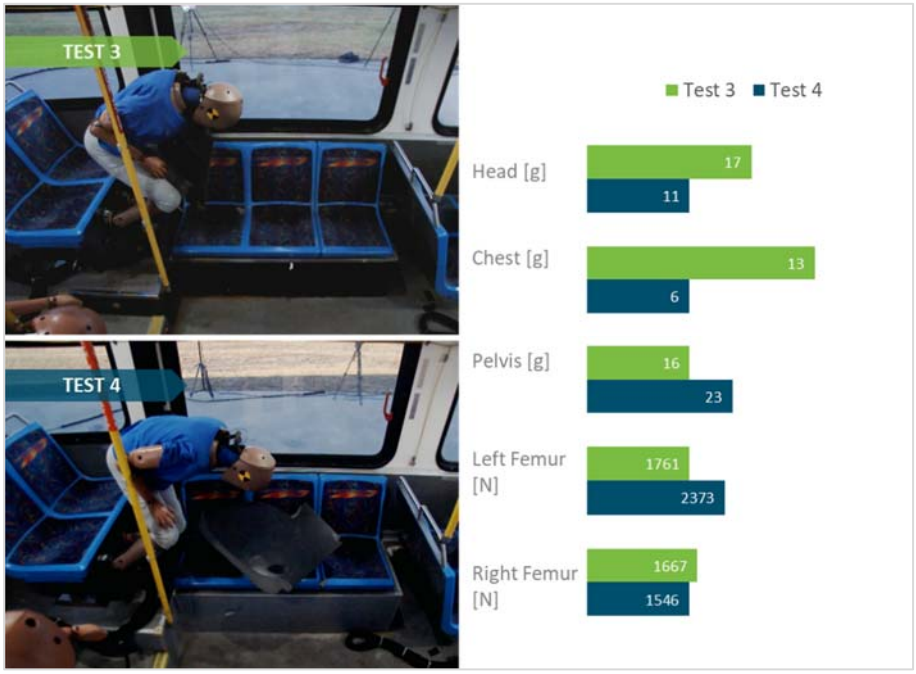

Figure 31: Freeze frames of the dummy seated in Position I in Tests 3 and 4 at the time of peak head excursion (left panel) and the peak head, chest, pelvis, and femur responses (right panel).

Figure 31 presents freeze-frames of the Hybrid III 5th percentile dummy placed in Position I. In both Tests 3 and 4, the knees of the dummy impacted the barrier and catapulted over the remaining structure of the barrier. The plastic panel fractured near one of its attachment points, slightly below the knees of the dummy. The upper half of the panel detached from the post and swung forward while the bottom half remained in place. Forward excursion of the dummy was greater in Test 4 than Test 3. The final resting positions are shown in Figure 32. In Test 3, the dummy had rebounded back into the seat and the face was in contact with the fracture edge of the remaining barrier. In Test 4, the dummy was suspended at the right elbow by the attachment fixture (centre photo) and at the left chest on the remaining structure of the barrier.

Figure 32: Photos of post test position for the dummy seated in location I for Test 3 (top) and Test 4 (bottom).

Figure 33: Freeze frames of the dummy seated in Position J in Tests 3 and 4 at the time of peak head excursion (left panel) and the peak head, chest, pelvis, and femur responses (right panel).

Figure 33 presents freeze-frames of the Hybrid III ten-year-old dummy placed in Position J. In both Tests 3 and 4, the knees of the dummy impacted the barrier. As the dummy pivoted over the barrier the left shoulder impacted the vertical hold bar. The panel flexed but did not break. As shown in Figure 34 the dummy in both tests came to rest suspended by the neck.

Figure 34: Photo of post test position for the dummy seated in location J.

The side-facing 5th percentile WorldSID (WS 5th) side impact dummy in the side facing rear row seat of the target bus was projected rearward. In both tests, shown in Figure 35, the dummy impacted the armrest with the left hip while the unrestrained upper body continued rearward.

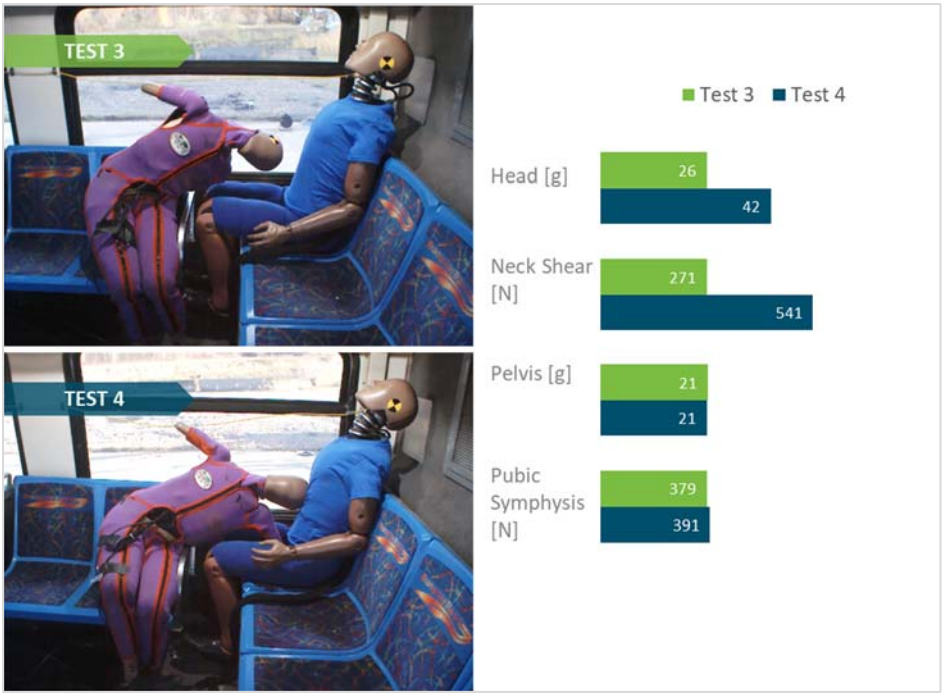

Figure 35: Freeze frame of the dummy seated in the target vehicle, Position K in Tests 3 and 4 (left panel) and the peak head, neck, and pelvis responses (right panel).

In Test 3, the 5th percentile side impact dummy was ejected from the seat and travelled towards the dummy seated in the rearmost position. The head of the WS 5th impacted the forward edge of the rearmost seat (adjacent to the Hybrid III 50th) before falling on the floor of the bus while in Test 4, the dummy contacted the Hybrid III 50th chest before falling to the floor.

In Test 3 and Test 4 the pelvis of 50th percentile dummy positioned in the rearmost forward-facing row of the Target Vehicle remained in place. The dummy moved towards the seatback, where only its head and neck were unsupported. The freeze frames in Figure 35 show a small increase in the hyperextension of the neck in Test 4.

3.2.4.3 Test 5

Freeze frame images and responses are presented for Test 5. The bus used in Test 5 was an inter-city type bus with high back seats and an interior layout that was quite different from the previous transit buses. Since a dedicated space was available, a Hybrid III 50th was installed in a wheelchair and secured with a lap-torso seatbelt.

The wheelchair was the only instance where there was no head contact and no ejection. Of the 16 other dummies placed in passenger seats, there were 13 head impacts and three partial ejections from the seat. A partial ejection means that the dummy was launched upward, out of the seat but did not land on the floor as for a complete ejection. Head impacts into a seatback or barrier were generally associated with elevated head accelerations while ejections and partial ejections were associated with peak head accelerations that occurred later and were not as elevated.

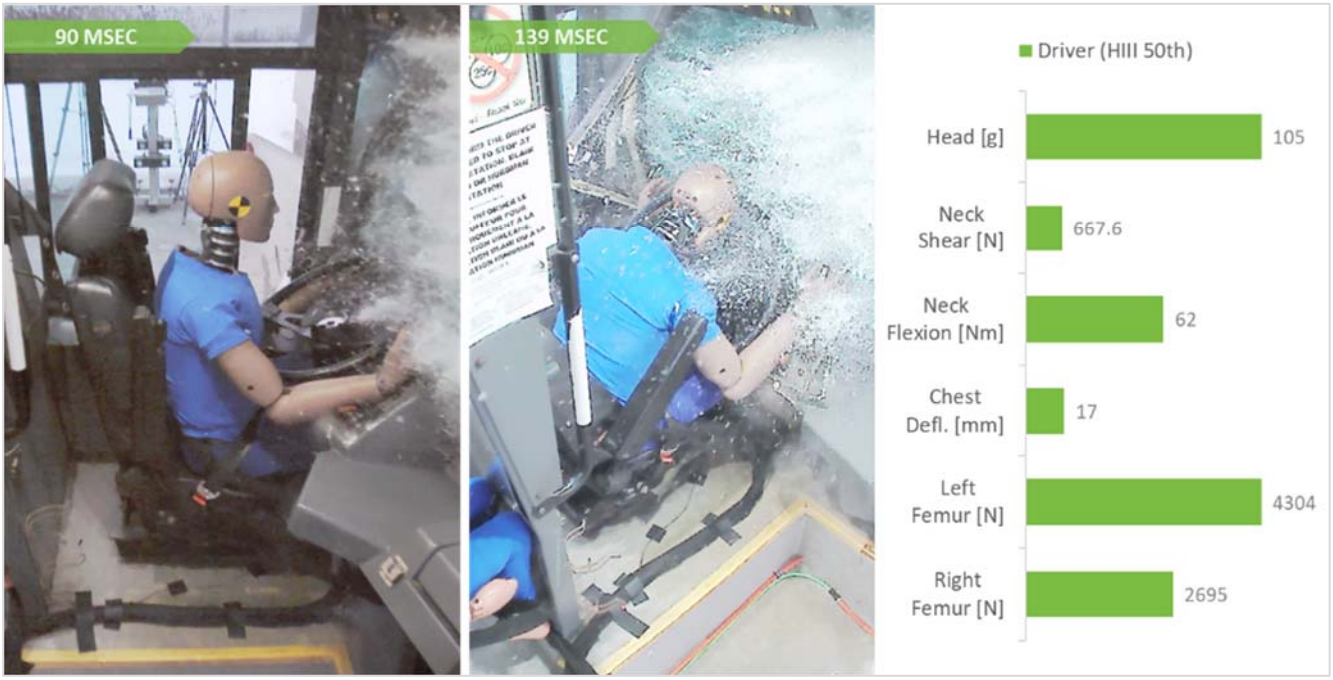

Figure 36: Freeze frame of the dummy seated in the driver seat, in Test 5 (left panel) and the peak head, neck, chest and femur responses (right panel).

Figure 36 presents freeze-frame image of the 50th percentile dummy at the time the head impacts the upper rim of the steering wheel. The dummy was restrained only by the lap belt. The dummy translated forward in an upright posture until, the lower rim of the steering wheel impacted the chest. The low chest deflection (17 mm) suggests that the rim impacted the chest below the sternum where the deflection is measured. The head and torso then continued to rotate about the steering wheel until the head impacted upper the rim resulting in a peak head acceleration of 105 g.

Figure 37 presents freeze-frame image of the HIII 10-year-old dummy at the time the face impacts the barrier. The dummy was observed to translate forward in an upright seated position, the strike the barrier first, the upper body tips forward and the face strikes the barrier. The second dummy seen in the left of the image is the 5th percentile side impact dummy. This dummy pivots over the seatback into the open space between the window and the 10-year-old dummy.

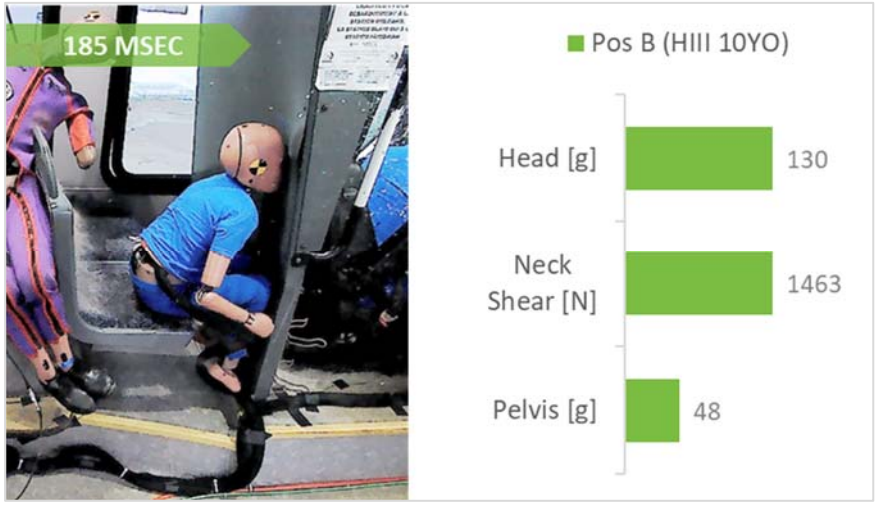

Figure 37: Freeze frame of the dummy seated behind the driver seat, in Test 5 (left panel) and the peak head, neck, and pelvis responses (right panel).

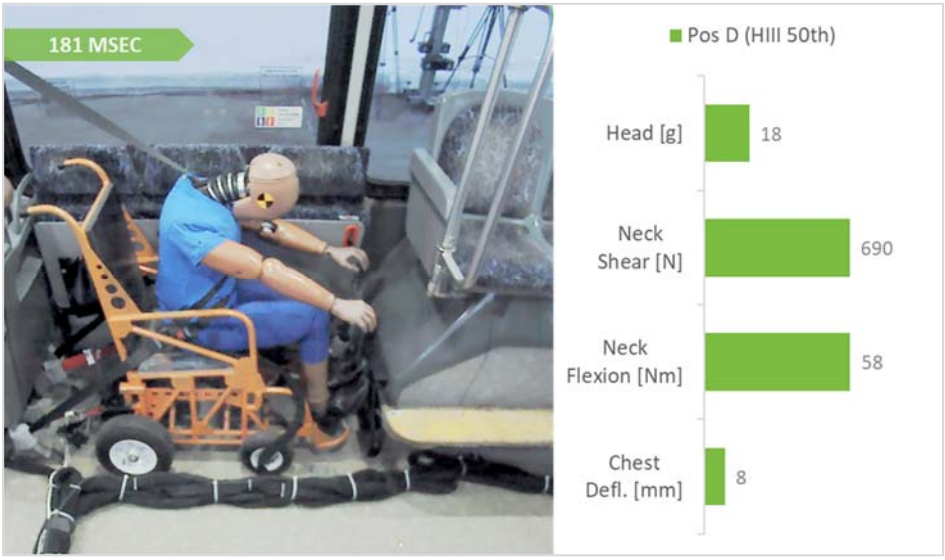

Figure 38: Freeze frame of the dummy seated in wheelchair, in Test 5 (left panel) and the peak head, neck, and chest responses (right panel).

The wheelchair, shown in Figure 38 was an ANSI/RESNA W18 surrogate wheelchair fabricated specifically for crash testing. The tie downs for the wheelchair controlled the forward motion of the wheelchair. The lap and shoulder belt restrained the HIII 50th dummy in the wheelchair. Dummy responses, including the chest deflection were low and no part of the dummy came into contact with its surrounding.

Figure 39 illustrates head contact with the rails of the luggage rack. Peak head resultant acceleration was 126 g with a calculated 3 ms acceleration clip of 116 g.

Figure 39: Freeze frame of the dummy seated at the front of the non-struck side of the bus, in Test 5 (left panel) and the peak head, neck, chest, and pelvis responses (right panel).

Figure 40 presents freeze-frame image two different types of six-year-old dummies that each respond quite differently. In the left image you see the head of the HIII 6-year- old (with the blue T-shirt) striking the hand rail/ top of the barrier. The 3ms clip for this head acceleration was 86 g. At the same moment the feet of Q6, in yellow, are loading the barrier and the knees are flexing. The dummy is then launched directly upward above the seat cushion as shown in the image to the right and eventually lands on top the hand rails of the barrier.

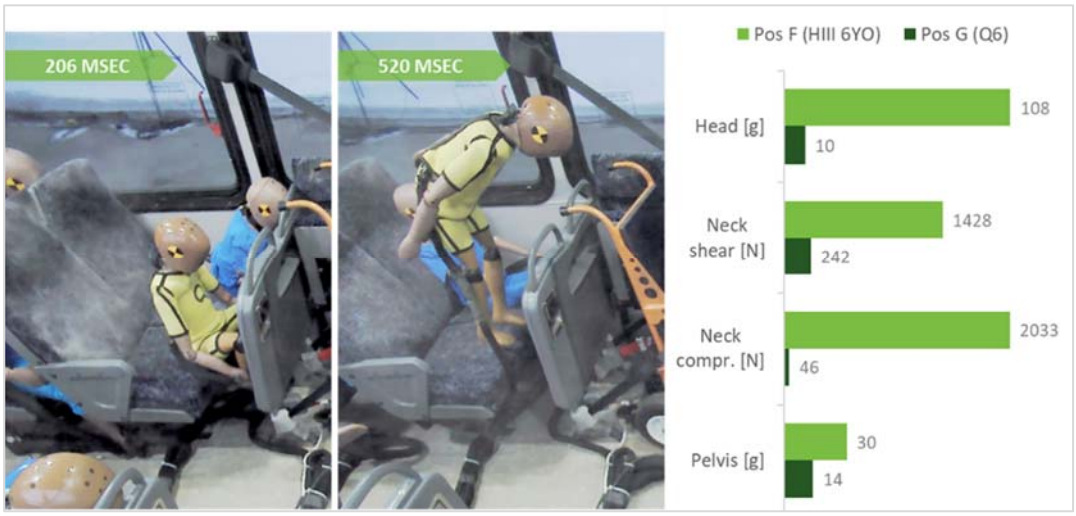

Figure 40: Freeze frame of the dummies seated behind the wheelchair, in Test 5 (left panel) and the peak head, neck, and pelvis responses (right panel).

Figure 41 to Figure 44 illustrate the interactions that occurred between different types and sizes dummies and the seat in front for both sides of the bus. Head impacts into the seat in front were observed in all seating locations on the lower level of the bus. The two dummies that were placed at the upper level rotated over the seats in front.

Figure 41 presents freeze-frame image two different types of ten-year-old dummies that each respond quite differently. The dummy in the foreground is the Q10. The top of the Q10 head impacts the handrail on the barrier, causing a large spike in the head acceleration. The 3 ms head clip calculated to be 56 g suggests that there was likely a hard contact between the head and the top edge of the barrier. The Hybrid III, shown in the background, impacted the flat surface of the barrier with the lower third of the face. This resulted in a lower acceleration peak but greater neck shear.

Figure 41: Freeze frame of the dummies seated across the aisle from the wheelchair, in Test 5 (left panel) and the peak head, neck, and pelvis responses (right panel).

Figure 42: Freeze frame of the dummies impacting seat in front in Test 5 (left panel) and the peak head, neck, and femur responses (right panel).

In Figure 43, both 6-year-old dummies impact the seat in front. The Q6 (in the yellow suit) slides to the floor of the bus following impact.

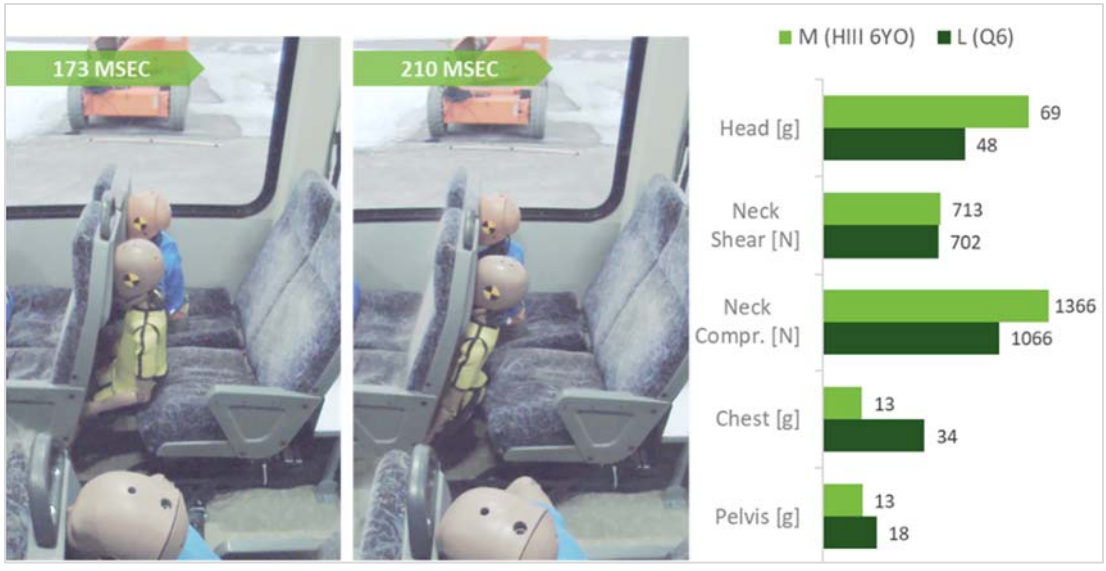

Figure 43: Freeze frame of the dummies impacting seat in front in Test 5 (left panel) and the peak head, neck, chest and pelvis responses (right panel).

Figure 44: Freeze frame of the dummies impacting seat in front in Test 5 (left panel) and the peak head, neck, pelvis, and femur responses (right panel).

3.2.5 Overview of All Dummy Responses

In the previous section, the responses of dummies were described in aggregate using the responses of a single dummy as a representative case. In this section, the responses of all of the dummies on board were treated independently. For each dummy, the responses in Tests 1 and 2 are presented in Table 2. Note that for the side-facing dummy, the neck response is the shear (measured in N), not bending moment (measured in Nm). The head acceleration reported is the peak resultant and not the 3 ms clip.

Table 2: Summary responses for each dummy on-board the striking vehicle in Test 1 and Test 2.

Dummy	Test No.	Head (g)	Pelvis (g)	Left Femur (N)	Right Femur (N)
Driver (50th percentile)	1	166	31	4 039	4 106
	2	54	24	966	1 472
Side-facing dummy (50th percentile)	1	33	11	–	–
	2	99	10	–	–
Row 1, Position B (10-year-old)	1	48	89	–	–
	2	20	97	–	–
Row 1, Position C (6-year-old)	1	37	105	–	–
	2	62	152	–	–
Row 2, Position D (5th percentile)	1	53	23	2 018	2 568
	2	71	28	2 586	2 456
Row 2, Position E (5th percentile)	1	67	18	1 620	2 157
	2	64	20	1 964	2 390
Row 3, Position F (5th percentile)	1	54	28	2 463	1 741
	2	71	36	2 065	2 761
Row 3, Position G (6-year-old)	1	61	59	–	–
	2	88	95	–	–
Row 4, Position H (50th percentile)	1	21	15	2 369	2 565
	2	48	15	2 687	2 743
Upper level, Position I (5th percentile)	1	6	21	2 125	1 809
	2	7	22	4 006	2 355
Upper level, Position J (10-year-old)	1	11	20	1 053	1 500
	2	12	15	1 235	1 079

The responses of the driver dummy were consistently lower in Test 2 than in Test 1. By contrast, the responses of all other dummies were generally greater in Test 2 than in Test 1.

Percentage changes for each dummy response were computed and are detailed in the Appendix. Percentage changes of at least 30 % were more frequent at the head and neck than in the lower body regions. Eight of the 11 head responses (~73 %) showed percentage changes between Tests 1 and 2 of at least 30 %. By contrast, only two of 11 pelvis responses (~18 %) and two of six femur responses (~33 %) showed percentage changes of at least 30 % between the two tests.

The responses of all of the dummies for Test 3 and Test 4 are presented in Table 3. Note that for the side-facing dummies in position A and K, the upper spine accelerometer was used to compare to the chest accelerometer in other dummies. The head acceleration reported is the peak resultant and not the 3 ms clip.

Table 3 Summary of responses for each dummy on-board the striking vehicle in Test 3 and Test 4.

Dummy	Test No.	Head (g)	Chest (g)	Pelvis (g)	Left Femur (N)	Right Femur (N)
1	3	23	24	44	-3673	-6784
50th percentile	4	25	18	59	-2956	-3337
A	3	131	55**	19	-	-
WS 50th percentile*	4	82	34**	15	-	-
B	3	25	18	55	-2054	-2117
six-year-old	4	70	32	52	-1578	-1216
C	3	35	27	87	-	-
ten-year-old	4	25	10	35	-	-
D	3	107	22	43	-	-
5th percentile	4	182	23	45	-	-
E	3	121	24	52	-2905	-2664
5th percentile	4	114	24	32	-2471	-3270
F	3	93	32	56	-	-
six-year-old	4	115	27	62	-	-
G	3	93	26	27	-2036	-2061
5th percentile	4	93	24	31	-2621	-2665
H	3	83	25	58	-	-
six-year-old	4	89	51	53	-	-
I	3	17	13	16	-1761	-1667
5th percentile	4	11	6	23	-2373	-1546
J	3	16	11	19	-1298	-951
ten-year-old	4	28	24	23	-1449	-1259
K	3	26	12**	21	-	-
WS 5th percentile*	4	42	14**	21	-	-
L	3	17	4	11	-542	-642
50th percentile	4	23	6	13	-606	-506

* WS: WorldSID side impact dummy

** The T4 resultant acceleration is reported

3.3 DISCUSSION

This research programme was designed to examine the effects of structural stiffness and energy management on the protection of transit bus drivers and passengers during frontal crashes. Five tests in total were conducted. Of these, two pairs were configured to provide a direct comparison of a bus that had not been modified to one that had had the front left corner or driver side of the bus strengthened. The strengthening, while not representative of a practicable or indeed achievable countermeasure was intended to add structural resistance in the crash zone.

In both pairs of tests, the strengthening reduced intrusion into the driver occupant space. As a result, the loads to the dummy were either reduced or redirected. Two different bus models were used for each matched pair. In the first pair of tests, the acceleration recorded in Test 2 at the centre of gravity (CG) of the Striking Vehicle (strengthened) and at each occupied seating location increased by less than 2 g; in the second pair (Test 4) the accelerations of the Striking Vehicle dropped by 1.2 g or less. The visual observations of deformation, 3D point streams, and accelerometer data, suggest that the energy of the impact was absorbed in large part through the structures surrounding the front left wheel. It would appear that in this model of bus less energy from the collision was transferred to the passenger compartment. Designs of this this type that allow the driver compartment to be strengthened to limit intrusion without transferring the collision energy to the passenger compartment could be beneficial to the driver and the passengers. For unbelted and standing passengers, even a 1 to 2 g difference can make a difference.

In all five tests peak accelerations at the CG and on the floor beneath occupied seats were below 10 g. The only exception was in test 5 where accelerometers installed at the driver location and on the floor at location B, behind the driver recorded peak accelerations that ranged from 12 to 17 g. The accelerometers in the driver compartment were disrupted by the deforming structures in the paired tests so the data could not be used.

A complete suite of crash test dummies was positioned in various passenger seat locations. The dummies ranged in size from an average sized 6-year-old to an average sized man, and included some of the latest generation dummies such as the THOR 5^{th} , the WorldSID 5^{th} and the WorldSID 50^{th}. It should be noted that all these dummies were designed to evaluate crash protection in passenger cars that are equipped with occupant restraints. In the passenger car, the dummy motion is constrained and the crash pulse is typically much more severe, 30 to 40 g. Since the dummies are designed to provide measurements (and withstand) in high energy crash test environments the upper body and limbs are necessarily stiff. Therefore, when used in the transit bus environment, the analysis of dummy responses must take into consideration the motion of the dummy and contact points that are captured with the high-speed video views. For example, differences in the responses were observed for the 10-year-old seated in location C of Test 3 and Test 4. Review of the videos indicated that a small change in the trajectory of dummy in Test 3 caused the right arm to get caught/ wedged in the seat in front. The final resting position of the dummy that was shown in Figure 27 is clearly not humanlike. However, while we may debate the validity of the sensor output and the poor similitude to humans, it is hard to imagine that this kind of outcome would not be associated with an increase risk of injury. The stiff legs posed yet another challenge when investigating lower leg injury mechanisms. Impacts between the lower legs and bottom frame of the seats in front were observed in the videos. Certain dummies included instrumentation in the lower legs but the data were not included because the upper leg, which is essentially a rigid steel tube acted as a blocker and interfered with the interaction of the lower leg and the seat structure.

Figure 45 compares the frequency of head impacts and ejections (partial or complete) for the five tests. The numbers represent the peak resultant head accelerations (g). Dummies that were placed in the elevated seats in the rear portion of the bus tore through the barrier and/or were thrown over the barrier or the seat back in front (Test 5). This suggests that in certain frontal crashes, the barrier, as tested, may not be sufficient to prevent occupant displacement into the forward space and subsequent occupant-to-occupant interaction. Furthermore, the exposed hardware used to secure the barrier in place that was shown in Figure 32 (bottom left photo), Test 3 Location I, could expose a human passenger to a risk of soft tissue injury, i.e., laceration, that cannot be detected by the dummy.

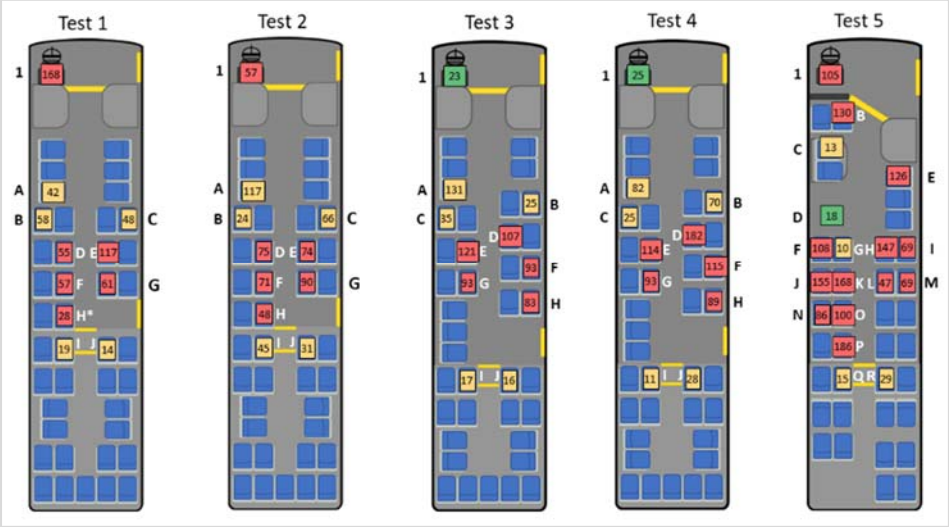

Figure 45: Seat locations where head impacts with the seat or barrier in front were observed (red) and where ejections from seats were observed (yellow).

All dummies on the lower lever, that had a seat back in front or as in the case of location B in Test 5, a full barrier in front, had head strikes. The locations are designated in red in Figure 45. The orientation of the head, the point of contact and the trajectory of the dummy are variables that may have contributed to the magnitude of the resultant head accelerations. In location H of Test 1, the dummy neck struck the hand rail, and the head cleared the handrail. As will be presented in the finite element modelling section, there is no instrumentation that is currently available to allow for the measurement of contact loads to the neck.

All other dummies with the exception of the dummies in the driver seat or in the wheelchair were either partially ejected or fully ejected and landed on the floor. The peak head accelerations identified in the yellow boxes as well as other dummy measures tended to be lower than the responses of dummies that remained or returned to their seats. This is likely due to the orientation of the instrumentation. In the Hybrid III, THOR and Q dummies the instrumentation is oriented to measure in the fore-aft direction. If a dummy is launched out of the seat and thrown to the floor the instrumentation may not be adequate to record the true response. Another consideration is that none of the current dummies can be used in a standing position or indeed in any position other than an upright seated position. It was therefore not possible to investigate the injury mechanisms for passengers who may be standing or leaning forward, for example.

In a series of sled tests, Olivares[6] noted the possibility of head injuries due to passenger-to-passenger contact. Olivares also identified the head, neck, and femur as the primary injury regions. Martinez et al.[7] observed in sled tests that adult dummies contacted the seatback in front with their knees and struck the seat in front with the head. These findings appear to be consistent with accident analyses conducted by Edwards et al.[8], who noted that injured seated passengers were most likely to have contacted vertical and horizontal handrails. According to traffic studies published by the United States' Federal Transit Administration[6,8], over half of bus occupant fatalities between 1999 and 2003 were attributed to non-ejected fatal impacts (53.8 %), almost double the fraction of fatalities attributed to ejection (28.2 %).

Despite all of the limitations of the current crash test dummies that have been presented, the results suggest that several interior structures such as grab handles and seatbacks could be a source of injury, even in a low to moderate collision. Currently, there are no specific requirements designed to manage injury risk associated with contact on these hard structures. By comparison, in passenger vehicles, several regulations and technologies exist to reduce the force of contact with hard interior surfaces of the vehicle. C/FMVSS 201 "Occupant protection in interior impact", for example, prescribes a test protocol and defines injury criteria for head impacts with instrument panels, and requires the use of energy-absorbing materials for sun visors and armrests.

4. SLED TESTS

4.1 CONSTRUCTION OF THE SLED BUCK

A sled buck representing a section of a transit bus passenger compartment was constructed so that, through controlled sled testing, the dummy responses could be understood in greater detail. Sled tests provide the advantage of high repeatability and low incremental cost per test, thus allowing precise, highly replicable, and wide-ranging experimentation.

The advantages that sled testing can offer—reproducibility and low incremental cost—are contingent on the fact that the buck, provided it is sufficiently rugged, can withstand repeated use without damage or wear. To ensure that the frame would be sufficiently rugged, the frame was constructed with 2"x4" steel tubes, the back of the frame was braced by additional 2"x4" tubes, and the joints were braced with 2"x2" tubes and 3/8"-thick plates.

The frame was designed and fabricated to allow experimentation with different seat configurations, seat types and interior structures. While the seats currently installed are from the OC Transpo New Flyer buses, other bus seat models may be attached instead. The spacing between rows of seats can be varied, and vertical posts can also be replaced or moved along the length of the buck.

The open frame of the buck maximizes light exposure and optimizes high-speed video views. Tubes extending outward from the length of the frame provide rigid supports and placement options for camera mount positions. In Figure 46, five high-speed cameras are mounted on the frame to record front and side views of the dummy motions. Three additional off-board cameras provide a top view and overall lateral views.

Figure 46: Front and side views of the bus buck attached to the deceleration sled bed.

4.2 SLED TESTS – PRELIMINARY SERIES

A preliminary series of 13 sled tests were conducted with the following objectives:

1. Verify whether dummy motions observed in the bus crash can be reproduced on the sled;
2. Identify the range of pulse severity that can be used to compare dummy responses without causing damage to the neck of the dummies during repeated test runs;
3. Describe how dummy characteristics and positioning can influence the measurement of injury mechanism

Sled tests were conducted using the sled buck described in the previous section. The seats, seat anchorages, and posts were taken from the OC Transpo buses. Each test employed one Hybrid III 5th percentile and one Hybrid III 50th percentile dummy in the second- and third-row seats. Neck shields were not used in sled tests so that the location on the neck where hand rail contact occurs could be visualized and recorded. The 3D positions of the dummies were recorded to precisely repeat dummy positions between tests.

Two deceleration pulses were used to investigate the influence of pulse severity on dummy responses: a moderate severity pulse with a peak acceleration of 6.5 g, and a lower severity pulse with a peak acceleration of 5.7 g. Both pulses were scaled from the acceleration recorded at position F aboard the striking bus in Test 1 (peak of 7.0 g) to reduce the risk of damaging the dummies.

Other than pulse, three additional test parameters were varied to investigate how the dummy positioning could influence the measurement of injury mechanism:

- **Occupied seat side (inboard or outboard):**

  Since the hand rail was 50 mm lower on the outboard side (near the window frame) than on the inboard side (far from the window frame), outboard-seated dummies were hypothesized to interact with the hand rail differently than inboard-seated dummies.

- **Dummy posture (reclined or upright):**

  The posture of the dummy determines the position of the knees relative to the seatback and the position of the head relative to the hand rail. Differences in dummy posture may therefore influence the knee-seatback and head-hand rail interactions. To investigate the potential effects of posture on dummy motions, dummies were installed with two different postures. In the reclined posture, the dummy's upper back touched the back of the seat it occupied, and a gap was present between the lower back and the back of the seat. In the upright posture, the dummy's upper back did not touch the back of the seat it occupied, and the lower back contacted the back of the seat.

- **Seating order (5th percentile in front or 50th percentile in front):**

  Potential effects of seating order were also considered to investigate if rear loading by the dummy placed in row 3 could influence the response of the dummy seated in row 2.

The test matrix is shown in Table 4. In each test, dummies were either both reclined or both upright.

Table 4: Test matrix for preliminary sled test programme.

Seating Position	Pulse and Posture			
	Moderate Pulse Severity		Low Pulse Severity	
	Reclined	Upright	Reclined	Upright
Out-board / In-board Row 2: [ ] [5th] Row 3: [ ] [50th]	3	1	1	1
Out-board / In-board Row 2: [ ] [50th] Row 3: [ ] [5th]	1	1	-	-
Out-board / In-board Row 2: [5th] [ ] Row 3: [50th] [ ]	1	1	1	1
Out-board / In-board Row 2: [50th] [ ] Row 3: [5th] [ ]	1	-	-	-

For both dummies, the sled test conditions that were most similar to the bus crashes were those with the moderate severity pulse, inboard seating positions, and similar postures (reclined for the 5th percentile; upright for the 50th percentile). On the sled, the reclined 5th percentile dummy contacted the seatback with its knees, which was generally followed by chin contact with the hand rail and rearward neck bending. The upright or non-reclined 50th percentile dummy contacted the seatback with its knees, the neck contacted the hand rail, and the neck flexed forward. These motions were comparable to those observed in Test 1. The similarity of dummy motions between the bus crashes and the sled tests suggests that the dummy motions observed in the buses can be reproduced on the sled.

Between tests of different pulse severity, the 5th percentile dummy's point of contact with the hand rail was comparable. As an example, the freeze frame images in Figure 47 reveal that the 5th percentile dummy, while seated inboard and reclined, contacted the hand rail with the chin in both the low and moderate severity tests. Similar to what was observed in Tests 1 and 2 of the bus crashes, the head and neck responses, increased in magnitude as pulse severity was increased.

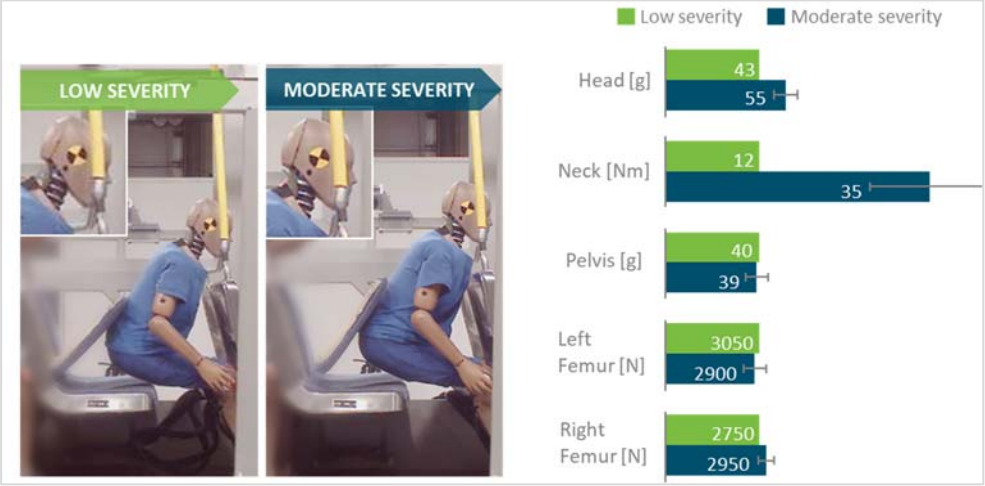

Figure 47: Comparison of freeze frame images of the 5th percentile dummy, seated inboard and reclined, on the sled at two pulse severities and the associated responses.

In contrast, it appears that for the 50th percentile dummy, as pulse severity increases, the point on the dummy body that impacts the rail shifts downward. For example, when seated inboard and upright, the 50th percentile dummy struck the rail at the upper neck in the low severity test and at the mid-neck in the moderate severity test. As a second example, the freeze frame images in Figure 48 indicate that the dummy, seated inboard and reclined, contacted the hand rail at the chin in the low severity test but at the neck in the moderate severity test. Since head contact occurred only in the low severity test, the head acceleration shown in the right side of Figure 48 decreased as pulse severity was increased.

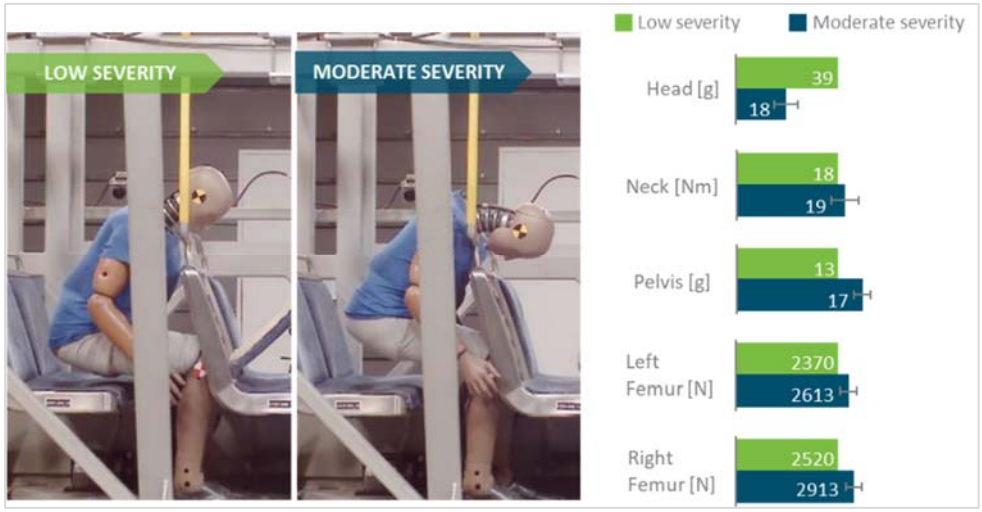

Figure 48: Comparison of freeze frame images of the reclined 50th percentile on the sled at two pulse severities and the associated responses.

As previously described, in low severity tests, the reclined 50th percentile dummy contacted the hand rail at the chin, whereas contact occurred at the neck when the dummy was seated upright. Therefore, posture appears to influence the responses of the 50th percentile dummy. The point of contact for the 5th percentile dummy was similar between both postures. Seating order was not associated with noticeable differences. Further testing, possibly with different seat models, is required to better understand how seat loading from the rear dummy could influence the dummy responses.

Seating the dummies on the outboard side rather than the inboard side led to interactions between the dummy and hand rail that were not seen on the inboard side or in the bus crashes. On the outboard side, the hand rail was 50 mm lower than on the inboard side, and accordingly, contact with the hand rail occurred lower on the dummy on the outboard side. In 3 of the 5 outboard tests, the 50th percentile dummy contacted the hand rail at the upper chest (as shown in the right panel of Figure 49) rather than the neck or chin. In all outboard tests, the 5th percentile dummy contacted the hand rail at the neck instead of the chin, and the dummy neck bent forward instead of rearward (Figure 49). The responses of outboard- and inboard-seated dummies must both be considered in order to develop a rigorous test protocol that is inclusive of all seating positions.

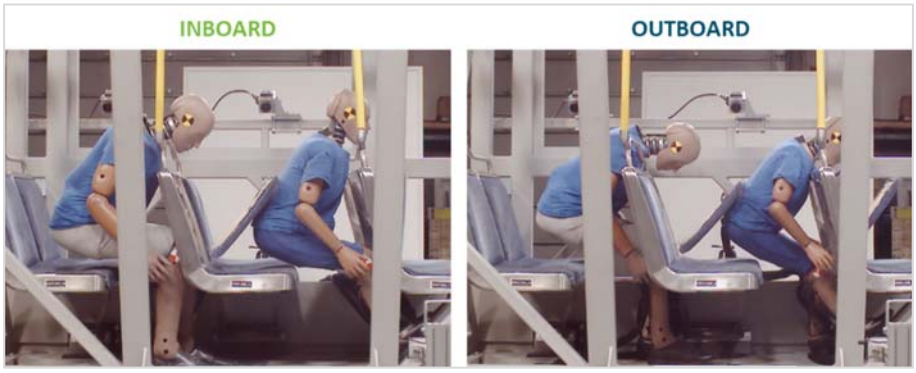

Figure 49: Comparison of freeze frame images for the 5th and 50th dummies in the inboard vs. outboard seating locations.

Based on the observed dummy motions, dummy characteristics that may influence the observed injury mechanisms are the stiffness of the neck and spine as well as the seated pelvis shape. These characteristics limit the ability of the dummy to respond in a humanlike manner as it translates forward, rotates, and interacts with the seatback and hand rail. As a result, the subsequent interpretation of injury mechanism or severity, which are based on the dummy responses, may be inaccurate. A more precise understanding of the how the dummy characteristics influence its motions and measured kinematic and kinetic responses is required to develop robust test methods that appropriately consider the capabilities and limitations of the dummy in unrestrained bus environments.

5. FINITE ELEMENT ANALYSIS

In the full-scale bus tests and the sled tests, the stiffness of the dummy neck and spine were suspected to limit forward rotation and misrepresent interactions with the seatback in front. A simulation study was conducted by Christopher Pastula at the University of Waterloo to examine how finite element human body models (HBMs), when used in tandem with physical test results, may contribute to a more accurate prediction of injury mechanisms for the transit bus environment.

5.1 OBJECTIVES

- Develop and validate a finite element model of the transit bus sled buck
- Compare simulated motions of 50th and 5th percentile HBMs on the sled buck to those of dummy models

5.2 BACKGROUND

5.2.1 Finite Element Modelling of Impact Scenarios

A finite element (FE) model is a virtual representation of a physical object used to predict its response to an applied load. Using FE models, impact scenarios can be simulated, with occupants represented either by FE models of crash test dummies or by FE human body models.

- **FE models of crash test dummies** serve as digital twins of the physical dummies. While computationally efficient and useful for exploration of design spaces, dummy models possess the same design limitations as their physical counterparts.
- **FE human body models (HBMs)** are more detailed representations of human bodies. HBMs include detailed characterizations of anatomical structures that dummies lack, such as bones, organs, and soft tissues. Additionally, unlike dummies, HBMs can be designed to model traumatic tissue failure responses, e.g., bone fracture.

Since HBMs do not possess the same design limitations as dummies, HBMs are useful for filling knowledge gaps present in physical testing due to dummy limitations.

5.2.2 GHBMC Human Body Models

The finite element HBMs used in this study were developed through the Global Human Body Models Consortium (GHBMC)[12], a group consisting of seven major automotive manufacturers and one manufacturer of safety systems. The GHBMC consolidates human body models of different body regions, each of which is developed by one of six Centres of Expertise. The models have been extensively validated under multiple impact scenarios, including frontal, lateral, and rear impacts, and are used by researchers in academia and industry.

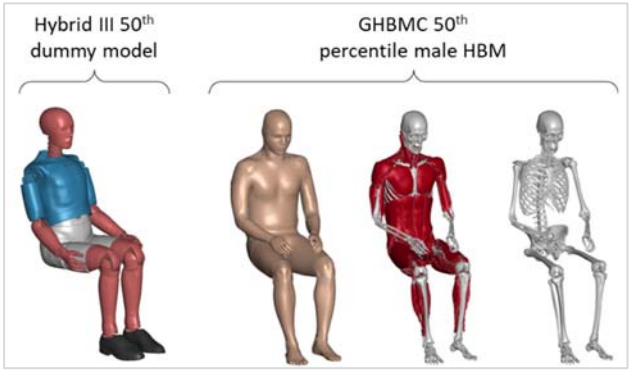

Figure 50: FE model of the Hybrid III 50th percentile dummy and the GHBMC 50th percentile male HBM.

5.3 METHODS

5.3.1 Construction of the Test Buck Model

The finite element model of the sled buck was constructed using precise 3D coordinates measured on the surfaces of the seats of the physical sled buck. This allowed a detailed reproduction of the seat and seat anchorage geometries. The mesh of the model was made to meet standard requirements set for finite element models used in crash impact scenarios.

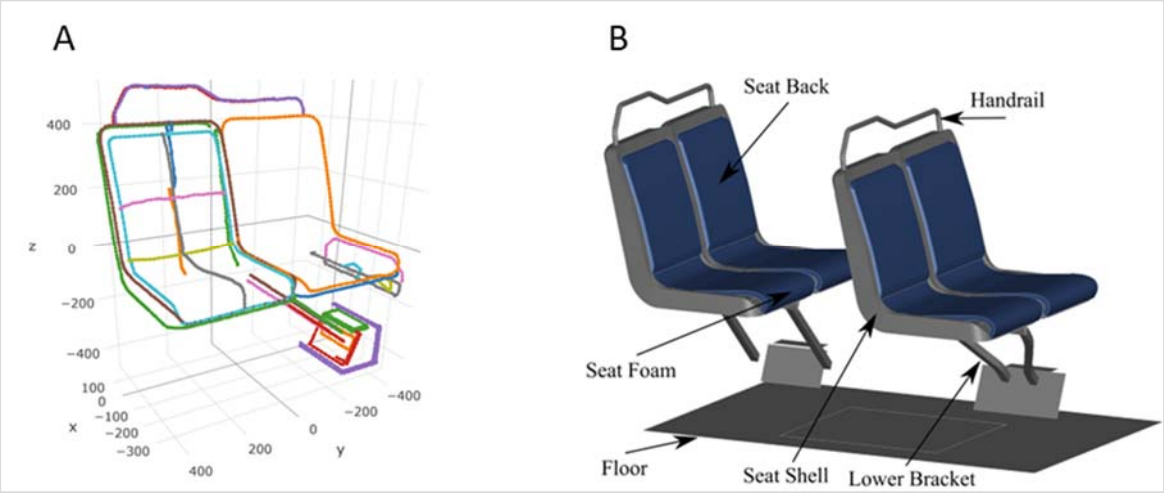

Figure 51: (A) Visualization of 3D coordinates measured on the surfaces of the physical seats and (B) finite element model of the seats.

5.3.2 Selection and Positioning of Occupant Models

In total, four different occupant models were used, each with a stature representative of an average (50th percentile) male or small (5th percentile) female:

- Hybrid III 50th percentile male dummy model
- Hybrid III 5th percentile female dummy model
- GHBMC 50th percentile male HBM
- GHBMC 5th percentile female HBM

The positions of the dummy models were matched to those of the physical dummies using measured pre-test coordinates of dummy features. The GHBMC models were repositioned to postures visually similar to those of the dummies.

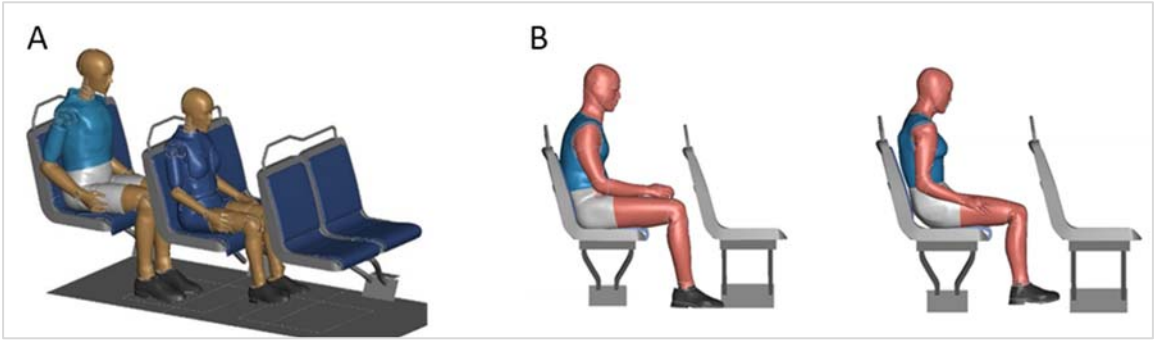

Figure 52: (A) FE models of the Hybrid III 50th and 5th percentile dummies and (B) the GHBMC 50th and 5th percentile HBMs positioned on the bus seats.

5.3.3 Validation of the Test Buck Model

The performance of the FE sled buck model was assessed according to how well the dummy models, when placed on the sled buck model, could predict the responses of the dummies recorded in the physical sled tests. The physical sled tests were conducted with the 50th and 5th percentile dummies while varying three test parameters:

- Seated side: outboard (near the window frame) or inboard (far from the window frame)
- Seated posture: reclined (gap between lower back and seatback) or upright (no gap between lower back and seatback)
- Magnitude of sled pulse: 6.5 g (moderate severity) or 5.7 g (low severity).

Eight experimentally tested combinations of seated posture, seated side, and pulse magnitude (referred to hereafter as conditions) were simulated using the 50th and 5th percentile dummy models (Table 5). One physical sled test was conducted in each condition except Condition #2 (in which three tests were conducted). In each simulation, the positions of the dummy models were matched to the measured pre-test dummy positions of the physical test conducted in the same condition.

Table 5: Combinations of tested conditions.

Condition No.	Pulse Magnitude (g)	Seated Side	Seated Posture	Number of Physical Tests Conducted
1	6.5	Inboard	Upright	1
2	6.5	Inboard	Reclined	3
3	6.5	Outboard	Upright	1
4	6.5	Outboard	Reclined	1
5	5.7	Inboard	Upright	1
6	5.7	Inboard	Reclined	1
7	5.7	Outboard	Upright	1
8	5.7	Outboard	Reclined	1

The predicted dummy motions of each simulation were qualitatively compared to the motions observed in the corresponding condition-matched physical test. Simulated kinematic and kinetic responses of the dummy models were quantitatively compared to responses recorded in the physical tests using the CORA rating method. CORA is an industry-standard method used to objectively rate model performance[13]. Through the CORA method, model performance is quantified as a CORA score, which is computed based on the correlation between simulated and experimental time-varying kinematic and kinetic responses. CORA scores range from 0 to 1, where 0 corresponds to no correlation between simulation and experiment, and 1 corresponds to perfect correlation. Based on the CORA score, the performance of the model can be categorized as poor, fair, good, or excellent.

Using the CORA method, each of the 10 physical tests specified in Table 5 were compared to the corresponding simulation run in the same condition. CORA scores were computed separately for the 50th and 5th percentile dummies. Each CORA score accounts for comparisons of nine time-varying kinematic and kinetic responses of the dummy (head acceleration, head angular velocity, neck force, neck moment, chest acceleration, chest deflection, pelvis acceleration, left femur force, right femur force).

5.3.4 HBM Simulations and Examination of Neck Impact on Handrail

Following validation of the sled buck model, the GHBMC HBMs were incorporated on the test buck model and subject to a simulated sled pulse. Because HBM simulations are more computationally costly to run than dummy simulations, one simulation each of the 50th and 5th percentile HBMs was run, both in the upright posture, seated inboard, and subject to the 6.5 g pulse.

The simulated motions of the HBMs were compared to those of the dummy models subject to the same test condition. Tissue-level HBM responses due to neck contact on the handrail were quantified as percentage compression of the larynx. In the literature, larynx fracture was reported to have occurred at compressions of 50% or more[17]. The contact forces on the dummy neck in simulations of the same condition were also extracted.

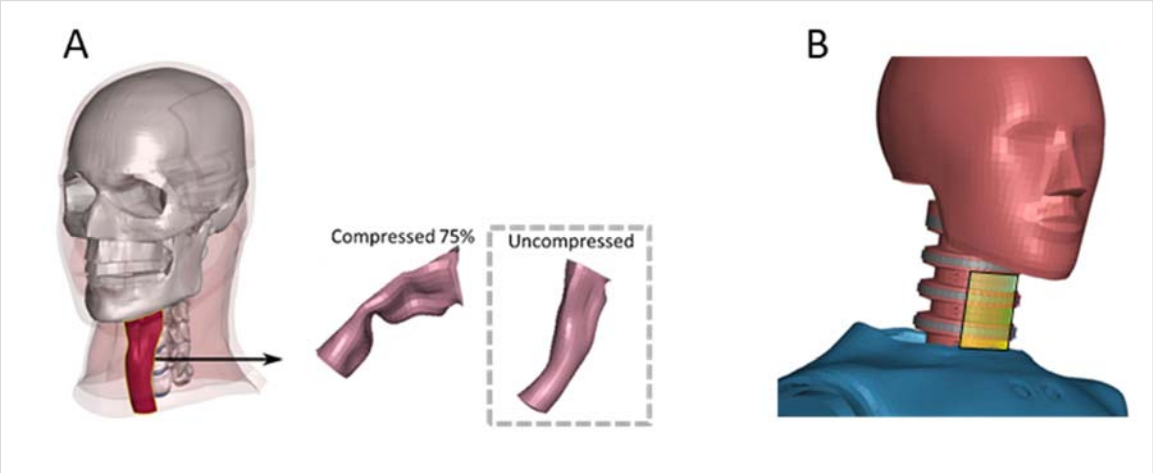

Figure 53: Responses to neck impact on the handrail, measured (A) on the GHBMC 50th percentile model as larynx compression, and (B) on the Hybrid III 50th percentile dummy model as contact force on the anterior neck.

5.4 RESULTS

5.4.1 Validation of the Test Buck Model

In all simulations, the 50th and 5th percentile dummy models each translated forward until the knees contacted the seatback in front. Both dummy models then pitched forward and contacted the handrail in front. The simulated motions of the 50th and 5th dummies were qualitatively similar to those observed in the physical tests.

An example comparison between the simulated 50th percentile dummy motion and the motion observed in the physical sled test is shown in Figure 54. Both the dummy model and physical dummy were seated upright on the inboard seat and subject to the 6.5 g pulse. Contact between the dummy knees and forward seatback occurred at approximately 121 ms in both the simulation and physical test. Then, in both the simulation and physical test, the dummy contacted the handrail at the mid neck at approximately 186 ms. In both the simulation and experiment, the neck flexed (bent forward) after contact with the handrail.

An example comparison between the simulated 5th percentile dummy motion and the motion observed in the physical sled test is shown in Figure 55. Again, both the dummy model and physical dummy were seated upright on the inboard seat and subject to the 6.5 g pulse. In both the simulation and physical test, the knees contacted the forward seatback, and the dummy pitched forward until the chin contacted the handrail. Contact of the chin on the handrail in both the simulation and physical test was followed by flexion (forward bending) of the neck. Chin contact on the handrail occurred approximately 20 ms later in the simulation than in the physical test.

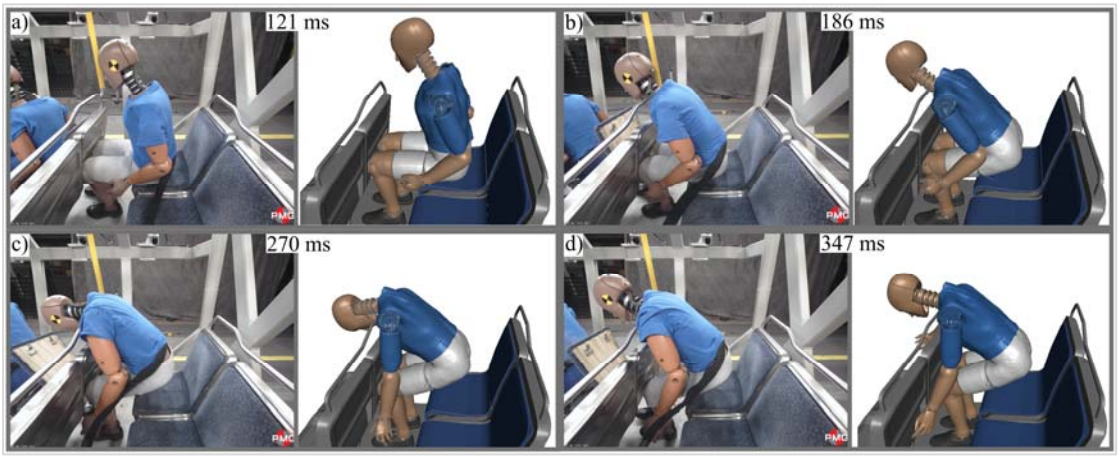

Figure 54: Visual comparison of motions between the physical Hybrid III 50th percentile dummy and its FE counterpart.

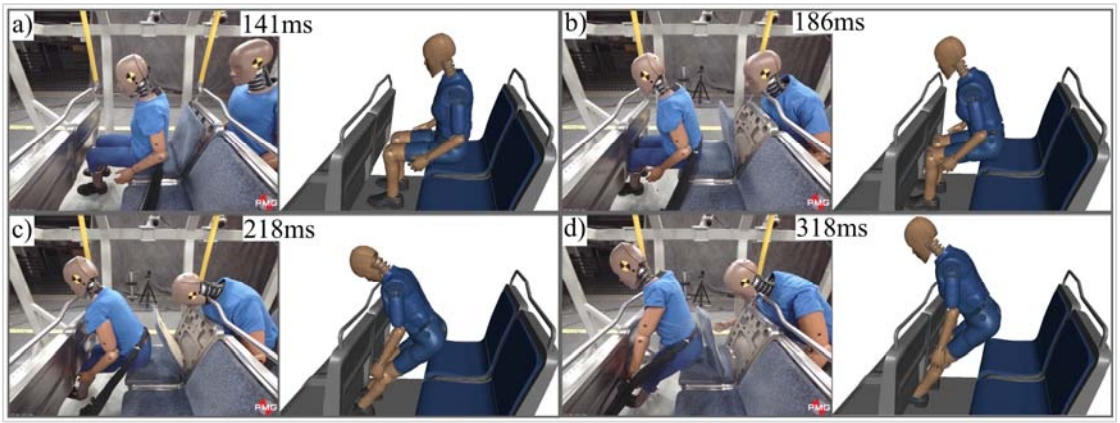

Figure 55: Visual comparison of motions between the physical Hybrid III 5th percentile dummy and its FE counterpart.

The performance of the sled buck model was quantitatively rated according to how well the dummy models, when placed on the sled buck model, could predict the kinematic and kinetic responses of the dummies recorded in the physical sled tests. The correlation between each simulation and its corresponding experiment was quantified by the CORA score, an industry-standard rating that ranges from 0 to 1, where 0 corresponds to no correlation between simulated and experimental responses, and 1 corresponds to a perfect correlation.

Using the CORA method, each of the 10 physical tests specified in Table 5 were compared to the corresponding simulation run in the same condition. CORA scores were computed separately for the 50th and 5th percentile dummies. In simulations of the 50th percentile dummy, CORA scores ranged between 0.674 (“good” rating) and 0.913 (“excellent” rating), with a mean of 0.779 (“good” rating). In simulations of the 5th percentile dummy, CORAs cores ranged between 0.45 (“fair” rating) and 0.719 (“good”) rating, with a mean of 0.634 (“fair” rating).

5.4.2 Predicted Motions and Contact Points of HBMs Differed from Those of Dummy Models

Simulated motions of the GHBMC 50th and 5th percentile HBMs were respectively compared to those of the Hybrid III 50th and 5th percentile dummy models. Multiple differences were identified, including:

- The 5th percentile HBM contacted the handrail at the lower anterior neck, whereas the dummy model of the same stature contacted the handrail at the chin;
- The spines of both HBMs were curved, whereas the rigid spines of the dummy models remained straight;
- For both HBMs, flexion of the spine and neck led to contact of the face on the top of the seatback, whereas the same contact was not predicted by the dummy models.

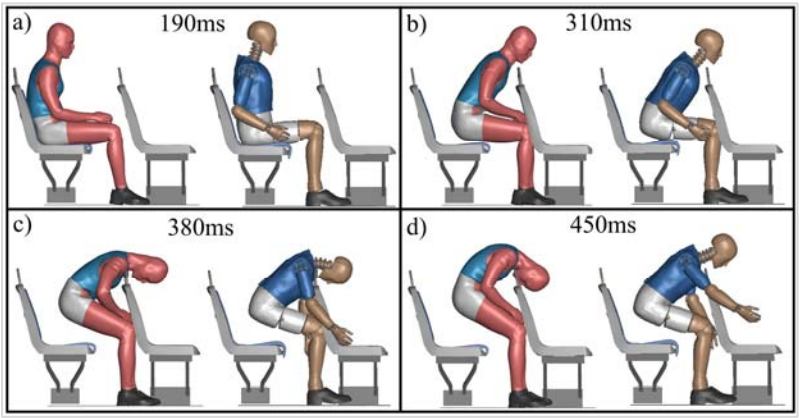

Figure 56: Visual comparison of motions between the 50th percentile HBM and the 50th percentile dummy model.

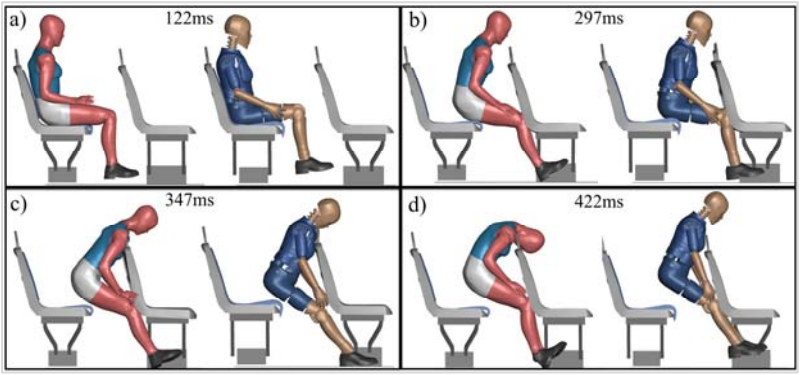

Figure 57: Visual comparison of motions between the 5th percentile HBM and the 5th percentile dummy model.

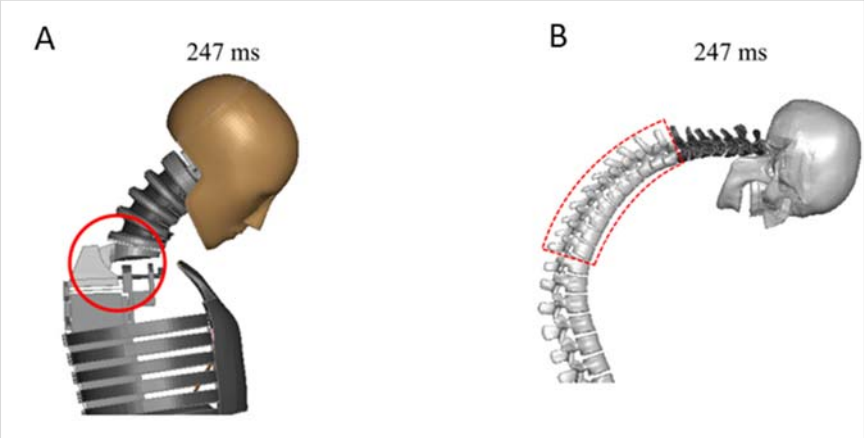

Figure 58: Comparison of the spines of the (A) 50th percentile dummy model and (B) 50th percentile HBM.

5.4.3 Neck Impact on Handrail in HBMs Was Associated with Injurious Levels of Larynx Compression

In the upright posture, inboard side, and 6.5 g pulse condition, contact of the neck on the handrail was observed of both HBMs as well as the 50th percentile dummy model. The resulting response at the neck was quantified as percentage larynx compression for the two HBMs and as neck contact force for the dummy model. Predicted larynx compressions were 75% and 80% for the 50th and 5th percentile HBMs, respectively. By comparison, larynx fracture was found in a literature source to have occurred at compressions of 50% or more[17]. In the same test condition, the predicted neck contact force of the 50th percentile dummy model was 300 N.

5.5 DISCUSSION AND CONCLUSIONS

- **An FE model of the sled buck was constructed, validated, and used to simulate impacts of the GHBMC HBMs in a transit bus environment.**
- **In a transit bus impact scenario, dummy limitations can influence the outcomes observed; certain dummy limitations can be elucidated through the use of HBMs.** In this study, focal impact of the neck on the handrail was predicted by the 5th percentile HBM but not the 5th percentile dummy model. The predicted larynx compression associated with neck impact exceeded levels reported in experiments to result in larynx fracture, highlighting the significance of the difference between HBM and dummy model responses. Larynx injuries and other blunt traumas of the neck have been reported to occur onboard buses[10,11,14,15,16]. However, we have not yet found detailed field data analyses in the literature that report the frequency and average severity of such injuries.
- **Additional HBM simulations using different test conditions, occupant models, and sled pulses should be conducted to supplement physical testing.** Focal impact on the neck is only one example of a potential interaction where the accurate prediction of occupant response is limited by a dummy that is not designed for the transit bus environment. In field data analyses of injuries sustained in bus collisions, the face and lower extremities were also found to be frequently injured[18].

6. RESEARCH RECOMMENDATIONS

The study has demonstrated that there are important opportunities to improve the protection of occupants in low to moderate severity transit bus collisions. Structural changes to the front of the bus were found to improve protection for the driver but did not improve the protection for the passengers. The transit bus crash tests highlighted the limitations of current crash test dummies when used for the evaluation of passenger protection regardless of seat placement while the use of a validated human body model was found to be a valuable adjunct to physical testing. In light of these findings the proposed crashworthiness research recommendations are the following:

1. The TC transit bus test buck should be made available to the industry to advance the development of interiors that will provide better energy absorption and improve commercial bus passenger protection;
2. Physical testing should be used in conjunction with numerical modelling to obtain a more complete description of the injury mechanisms and obtain a better approximation of the risk of injury;
3. Additional research should be conducted to advance the crash protection of transit bus drivers. Specific attention should be focused on limiting steering wheel and knee bolster intrusion.

7. REFERENCES

1. Statistics Canada. “Commuters using sustainable transportation in census metropolitan areas”. Internet: [https://www12.statcan.gc.ca/census-recensement/2016/as-sa/98-200-x/2016029/98-200-x2016029-eng.cfm], 2017-11-29 [2019-07-05].
2. Miller EJ, Shalaby A, Diab E, Kasrajan D. “Canadian Transit Ridership Trends Study”. Canadian Urban Transit Association, 2018.
3. Canadian Urban Transit Association (CUTA). “Canadian transit ridership continues to trend upwards”. Press release: [https://www.globenewswire.com/news-release/2019/11/13/1946490/0/en/Canadian-transit-ridership-continues-to-trend-upwards.html], 2019-11-13 [2020-10-22].
4. National Highway Traffic Safety Administration. “Traffic Safety Facts 2017”. 2017.
5. Transportation Safety Board of Canada. Railway Investigation Report R13T0192, 2015.
6. Olivares, G. Crashworthiness Evaluation of Mass Transit Buses. Federal Transit Administration Research, 2012, FTA Report No. 0021.
7. Martinez, L., Espantaleón, M., de Loma-Ossorio, M., et al. Adult and Child Dummies Tests for Safety Assessment of Seated Occupants in Urban Bus Collisions. Proceedings of the Enhanced Safety of Vehicles Conference, 2017, 17-0401.
8. Edwards, M., Edwards, A., Appleby, J., et al. Banging heads onboard buses: Assessment scheme to improve injury mitigation for bus passengers. Traffic Injury Prevention, 2019, 20(S1): S71-S77.
9. Hermann, T., Olivares, G. Mass Transit Crashworthiness Statistical Data Analysis. National Institute for Aviation Research, 2005, FTA Report No. 0002. (Executive Summary Figure)
10. AL-Njadat I, Obeidat M, EL-Sukkar W, AL-Swalgh M. “Isolated thyroid hematoma after blunt neck trauma presented with aphonia”. Med J. Armed Forces India, 2020; 76(4):456-458. doi: 10.1016/j.mjafi.2019.02.001
11. Chadwick DL. “Closed Injuries of the Larynx and Pharynx.” J. Lar. Otol., Lond, 1960; 74(5):306-324.
12. Gayzik FS, Moreno DP, Vavalle NA, Rhyne AC, Stitzel JD. “Development of the Global Human Body Models Consortium Mid-Sized Male Full Body Model”. Proceedings of the Thirty-Ninth International Workshop of Injury Biomechanics Research.
13. Gehre C, Stahlschmidt S. “Assessment of Dummy Models by Using Objective Rating Methods”. Proceedings of ESV Conference, 2011, Paper No. 11-0216.
14. Holinger PH, Schild JA, Maurizi DG. “Internal and External Trauma to the Larynx”. The Laryngoscope, 1968; 78(6):944-954. doi: 10.1288/00005537-196806000-00005
15. Juutilainen M, Vintturi J, Robinson S, Bäck L, Lehtonen H, Mäkitie AA. “Laryngeal fractures: clinical findings and considerations on suboptimal outcome”. Acta Otolaryngol, 2009; 128(2):213-218. doi: 10.1080/00016480701477636.
16. Kleinsasser NH, Priemer FG, Schulze W, Kleinsasser OF. “External trauma to the larynx: classification, diagnosis, therapy”. Eur Arch Otorhinolaryngo,. 2000; 257(8):439-444. doi: 10.1007/s004050000263.
17. Melvin JW, Snyder RG, Travis LW, Olson NR. “Response of Human Larynx to Blunt Loading”. Stapp Car Crash Journal, 1973. doi: 10.4271/730967.
18. Páez J, Furones A, Aparicio F, Alcalá E. “Spanish frontal accidents of buses & coaches. Injury mechanism analysis”. Proc Soc Behav Sci, 2014; 160(2014):314-322. doi: 10.1016/j.sbspro.2014.12.143